

NUS
National University
of Singapore

AIAA Design/Build/Fly
2016-2017
Design Report



Table of Contents

List of nomenclature widely used in this report:	4
1. Executive Summary	6
2. Management Summary	7
2.1. Team Organization.....	7
2.2. Milestone Chart	8
3. Conceptual Design.....	8
3.1. Mission Requirements	9
3.2. Analysis of Scoring Rubrics / Sensitivity Analysis.....	10
3.3. Design Requirements	12
3.4. Evaluations of Concepts and Configurations	12
3.5. Final Concept.....	16
4. Preliminary Design	18
4.1. Design Methodology.....	18
4.2. Lift Characteristics.....	19
4.3. Airfoil Selection	21
4.4. Drag Characteristics	24
4.5. Stability & Control.....	25
4.6. Propulsion Requirements	27
4.7. Mission Models	28
4.8. Estimated Mission Performance	30
5. Detail Design	31
5.1. Final Design Parameters	31
5.2. Structural Characteristics.....	32
5.3. Propulsion System.....	36
5.4. Weight & Balance.....	38
5.5. Rated Aircraft Cost	39
5.6. Computational Fluid Dynamics	39
5.7. Performance Characteristics of Final Design	39
5.8. Schematic Drawings	39
6. Manufacturing Plans	46
6.1. Milestone Chart	46
6.2. Material Selection	46

6.3.	Manufacturing Methods	47
6.4.	Manufacturing Components	48
7.	Testing Plans	51
7.1.	Testing Schedule	51
7.2.	Testing Methods	51
7.3.	Pre-flight Checklist	52
8.	Performance Results	53
8.1.	Test Performance Results	53
8.2.	Flight Test Results	55
8.3.	Area of Improvements	59
9.	Bibliography	60

List of nomenclature widely used in this report:

AIAA	- American Institute of Aeronautics and Astronautics
DBF	- Design-Build-Fly
CAD	- Computer Aided Drawing
FOM	- Figure of Merits
M1	- Score for Mission 1
M2	- Score for Mission 2
M3	- Score for Mission 3
Min_time	- Fastest Time to Complete 3 Laps of Any Team
N_time	- Time Taken to Complete 3 Laps by The Team
N_(laps*pucks)	- Value of (Laps*Pucks) by the Team
Max_(laps*pucks)	- Highest Value of (Laps*Pucks) of Any Team
Total mission score	- Sum of M1, M2, And M3
EWmax	- Maximum Aircraft Empty Weight
TW	- Tube Weight
L	- Tube Length
C	- Tube Circumference.
AR	- Aspect Ratio
AR _h	- Aspect Ratio of Horizontal Stabiliser
b	- Wing Span
S	- Wetted Wing Area
c	- Chord Length
ρ	- Air Density
α	- Angle of Attack
α_{\max}	- Maximum Angle of Attack
C _L	- Lift Coefficient
C _{L,0}	- Lift Coefficient at Zero Angle of Attack
C _{L,max}	- Maximum Lift Coefficient
C _d	- Drag Coefficient
C _{d,0}	- Drag Coefficient at Zero Angle of Attack
C _{d,i}	- Induced Drag Coefficient
e	- Span Efficiency Factor
V _v	- Vertical Tail Volume Coefficient
S _v	- Vertical Tail Area
I _v	- Vertical Tail Moment Arm
V _h	- Horizontal Tail Volume Coefficient
S _h	- Horizontal Tail Area
I _h	- Horizontal Tail Moment Arm
X _{np}	- Distance of Neutral Point from Leading Edge
X _{CG}	- Distance of Centre of Gravity from Leading Edge
B	- Lateral Stability

Y	- Dihedral Angle
W	- Weight
T _{av}	- Available Thrust
n	- Load Factor
θ	- Bank Angle
V	- Speed
V _s	- Stall Speed
V _{LOF}	- Takeoff Speed
V _{cruise, max}	- Max Cruise Speed
RAC	- Rated Aircraft Cost
MAC	- Mean Aerodynamic Chord
CG	- Centre of Gravity
CP	- Centre of Pressure
ESC	- Electronic Speed Controller
NiMH	- Nickel-Metal Hydride Battery
NiCd	- Nickel-Cadmium Battery
RC	- Radio Controlled
XFOIL	- 2D Airfoil Computational Software
XFLR5	- Analysis Tool for Airfoils, Wings and Planes

1. Executive Summary

Dart Vader team consists of 6 students from the National University of Singapore. This report documents the thought processes and actual tests performed by Team Dart Vader to design and build an aircraft to excel at the AIAA Design/Build/Fly 2016-2017 competition.

This year's competition requires us to create an aircraft that can be stowed within a tube, be deployed to flight position with self-locking mechanism and be hand launched into the air, instead of the conventional ground takeoff. There will be 3 different flight mission and 1 ground mission to be completed. The ground mission consists of dropping the tube with the plane inside from 12 inches of height onto a hard surface from three different angles, and the aircraft must not sustain heavy damage. The ground mission tests the aircraft on its structural strength and integrity. Hence, the stowing mechanism needs to be relatively strong. Flight mission 1 is to fly 3 laps without any payload, mission 2 requires us to fly 3 laps while carrying 3 pucks, and mission 3 tasks is to carry as many pucks as possible and fly as many laps as possible in 5 minutes. The mission score will be divided by the Rated Aircraft Cost (RAC), which consists of aircraft weight, and the tube dimensions and weight. The tube length must at least be 4 times of the tube diameter.

Through sensitivity analysis, the team determined that this year's emphasis is on creating the smallest possible aircraft in stowed configurations, without substantially compromising on structural strength, stability and maneuverability. Our team feels that the biggest challenge is to ensure that the aircraft has enough lifting capabilities to carry the payload, especially when hand launch speed is usually lower compared to a ground takeoff.

The solution that our team provides is a conventional aircraft with a rotating wing mechanism, long fuselage length, and a dual tail configuration. The rotating wing ensures that we maximize the space inside the tube and ensuring we have enough wing area to takeoff when fully loaded. The fuselage length is lengthened to allow the tail to be shrunk while maintaining decent stability. The dual-tail makes it easier for the plane to be fitted inside the tube. Therefore, the driving factor for the tube diameter and size will be the wing chord length.

Our team then prioritize making our aircraft as compact and light as possible, rather than trying to excel in the flight mission. Therefore, we have selected a relatively weak propulsion system; this is to minimize the weight caused by carrying powerful motor and batteries. The aircraft will carry the minimum number of pucks, 3, and design our wing area to be just enough that payload. This simplifies our mission tasks as mission 2 and mission 3 becomes similar, and we can design our aircraft based on the same requirements.

The rotating wing mechanism will be achieved by attaching two tubes into the wings where it will rotate about grooves that are cut on the fuselage; this allows the wing to be accurately deployed to the flight conditions as the groove will guide the wing to the correct spot and orientation. The tubes will then be secured in place using umbrella latch mechanism. The latch provided a one-way locking system in which we only need to push the tubes through the latch to lock it in place.

After undergoing a training phase to build a simpler RC plane, and going through many rounds of iterations. The team has constructed a working prototype that proved the feasibility of the mechanism and the aircraft's airworthiness. It has also undergone testing to ensure the capabilities of its systems and subsystems. We believe that we can create a competitive plane for the upcoming AIAA DBF Competition.

2. Management Summary

The Dart Vader team consists of three supervising professors and six students (three juniors and three sophomores), thus fulfilling the 1/3 requirement. The three supervisors guide the students, who are relatively inexperienced in the mechanics of flights and aerodynamics before this project.

2.1. Team Organization

Dart Vader uses a hierarchical structure to establish leadership and responsibilities within the various sub-teams to fulfill all the requirements to successfully participate in the competition. The workload was divided during the design phase into Structure, Aerodynamics, Propulsion, Control & Stability, Report Writing and Publicity & Corporate Relations. As the team is comparatively small, every member must be proficient in multiple disciplines. All team members participate in construction, testing, and report writing.

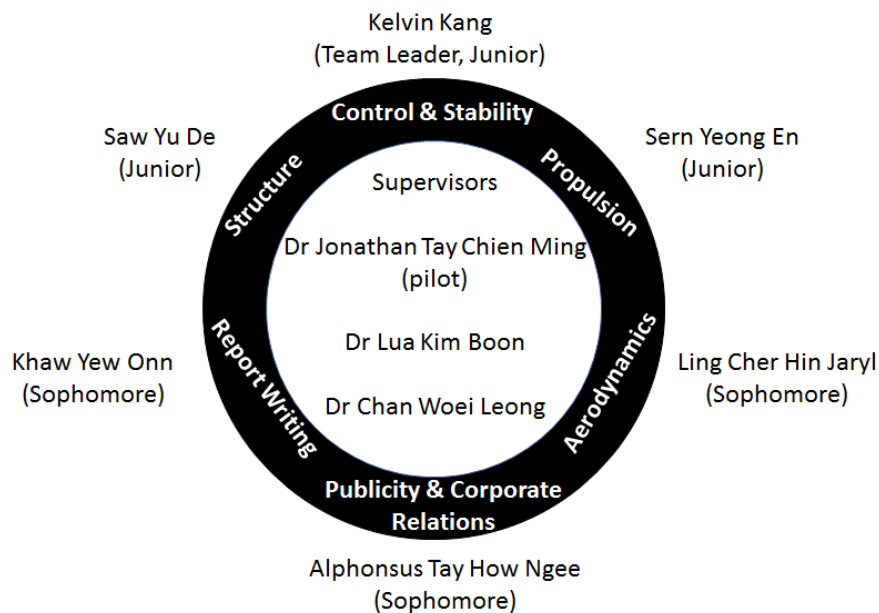


Figure 1: Organizational Chart

Designation	Roles and Responsibilities
Supervisors	Provide feedback to the team as they have the most experience in the field. Ensure feasibility of the plane design and manufacturing process.
Team Leader	Manages the tasks and responsibilities of each person and sub-groups to ensure that deadlines are met.

Aerodynamics Team	Analyze and determine the optimum aircraft configuration and airfoil to maximize the final score.
Propulsion Team	Analyze the power requirement of the airplane and design the propulsion system. Research and optimize our hand-launch methods and design considerations.
Structures Team	Select materials for the various parts of the plane and create CAD drawings. Plan and coordinate the manufacturing and assembly process of the aircraft.
Stability & Control	Design the servo connections for the control surfaces and electronic system.
Report Writing	Write the proposal and final report for our aircraft design.
Corporate Relations	Source & liaise with potential sponsors. Maintaining our media presence on social media platforms to gain publicity.

Figure 2: Roles & Responsibilities Table

2.2. Milestone Chart

A milestone chart is established at the beginning of the design process to capture major deadlines, design stages, and manufacturing goals. The team leader monitors the team's progress to ensure all key milestones are met. The team meets with the project supervisors at least once every week to discuss the team's progress as well as to receive feedbacks and ask for expert advice. The milestone chart is shown below in Figure 3, capturing both the planned and actual timing of major events.

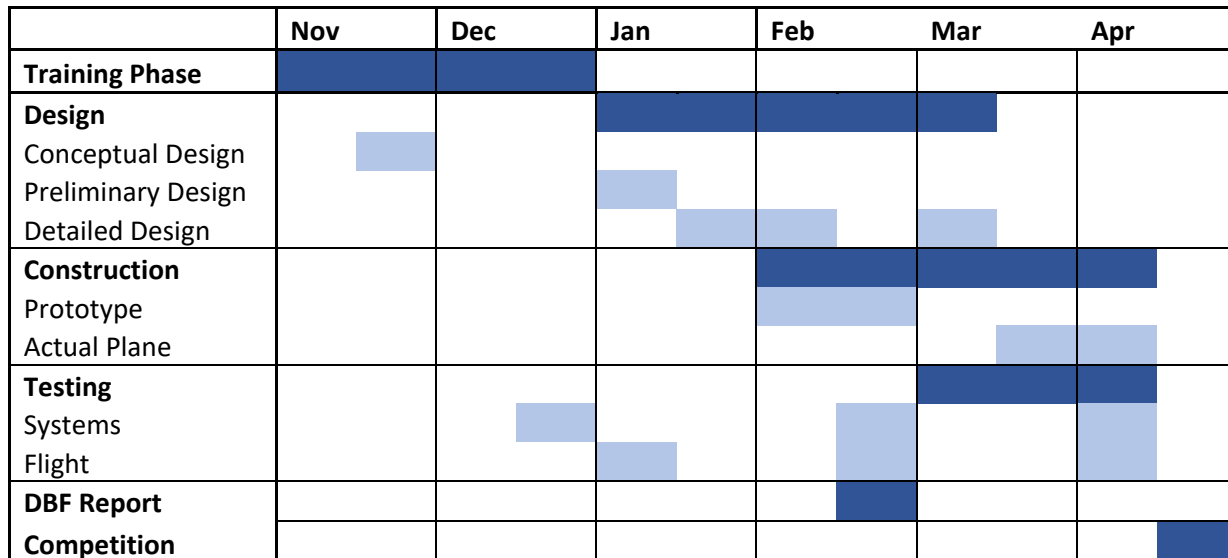


Figure 3: Milestone Chart

3. Conceptual Design

The conceptual design serves to translate the mission requirements into design requirements, analyze scoring rubrics and identify parameters that will maximize the performance score. We considered several aircraft configurations and represented it using FOM by taking into consideration the critical parameters

that were identified previously. The evaluation concludes with a design concept that prioritizes flight performance within the competition constraints.

3.1. Mission Requirements

3.1.1. General Requirements

The aircraft, its subsystem, and the launch tube must achieve certain design requirements as stated in the mission task matrix while minimizing system weight and maximizing flight performance. The team must take note of the following requirements:

- The aircraft must be stowed within a tube that provides sufficient protection to the aircraft during the all-aspect drop tests.
- Structural integrity and functionality of both tube and aircraft must not be compromised after the drop tests.
- All aircraft features must be secured with self-locking captive mechanical mechanisms when transiting from stowed to flight condition.
- The aircraft needs to be hand-launched by a single operator holding the fuselage.
- All battery used must be either NiMH or NiCd batteries.
- The aircraft must be able to carry a payload of at least three regulation hockey pucks.
- Three flight missions in total. (1) Complete 3 standard laps within 5 minutes while carrying no payload (2) Complete 3 standard laps with 3 hockey pucks (3) Complete as many laps with the maximum payload possible.

Missions must be accomplished in the following order. Failure to achieve a satisfactory landing will result in no score for that mission. The definition of a satisfactory landing is at the discretion of the site judges. The mission clock starts when the aircraft leaves the launcher's hand during the first attempt. The clock stops exactly 5 minutes later, or upon mission completion, or catastrophic failure of the aircraft, whichever occurs first.

3.1.2. Flight Requirements for Mission 1

M1 = 1.0 for successful mission

The team must complete 3 laps without any payload within 5 minutes. A lap is complete when the aircraft passes the finishing line in the air. Failure to land will result in zero scores. Figure 4 shows the standard course layout for all the missions.

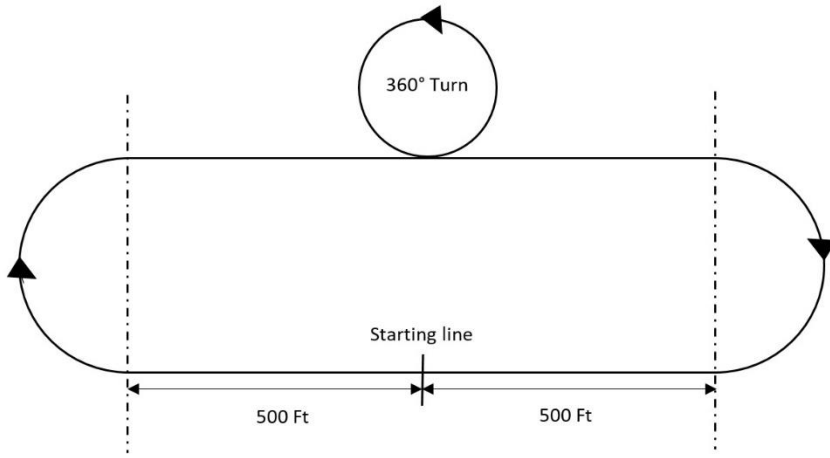


Figure 4: Course Layout

3.1.3. Flight Requirements for Mission 2

$$M2 = 2 \times \frac{\text{Min_time}}{\text{N_time}}$$

The aircraft has to carry 3 regulation hockey pucks internally within the aircraft and complete 3 laps.

3.1.4. Flight Requirements for Mission 3

$$M3 = \frac{4 \times N_{\text{(laps}} \times \text{pucks)}}{\text{Max}_{\text{(laps}} \times \text{pucks)}} + 2$$

The team is required to carry any number of hockey pucks internally within the aircraft and fly as many numbers of laps. The score will be the multiplication of the number of pucks and laps.

3.1.5. Requirements for Ground Mission

The aircraft must first pass the wing tip loading test with the maximum flight payload during the tech inspection. The team must conduct 3 drop tests which involve lifting the launch tube with the aircraft inside to a minimum height of 12 inches and dropping it onto a hard surface. The 3 drop tests refer to a flat drop (axis parallel to the ground), and 2 opposite end drop (axis perpendicular to the ground). Structural integrity must not be compromised. The team will then remove the aircraft from the tube and transit to flight condition to verify that controls and subsystems are functional. Any significant damage to launch tube or aircraft will result in failure of this mission.

3.2. Analysis of Scoring Rubrics / Sensitivity Analysis

The factor considered for the AIAA DBF 2016-17 scoring includes 3 flight missions and a written report. The formula used to compute the score is shown below:

$$\text{Score} = \frac{\text{Written report score} \times \text{Total mission score}}{(\text{EWmax} + \text{TW}) \times (\text{L} + \text{C})}$$

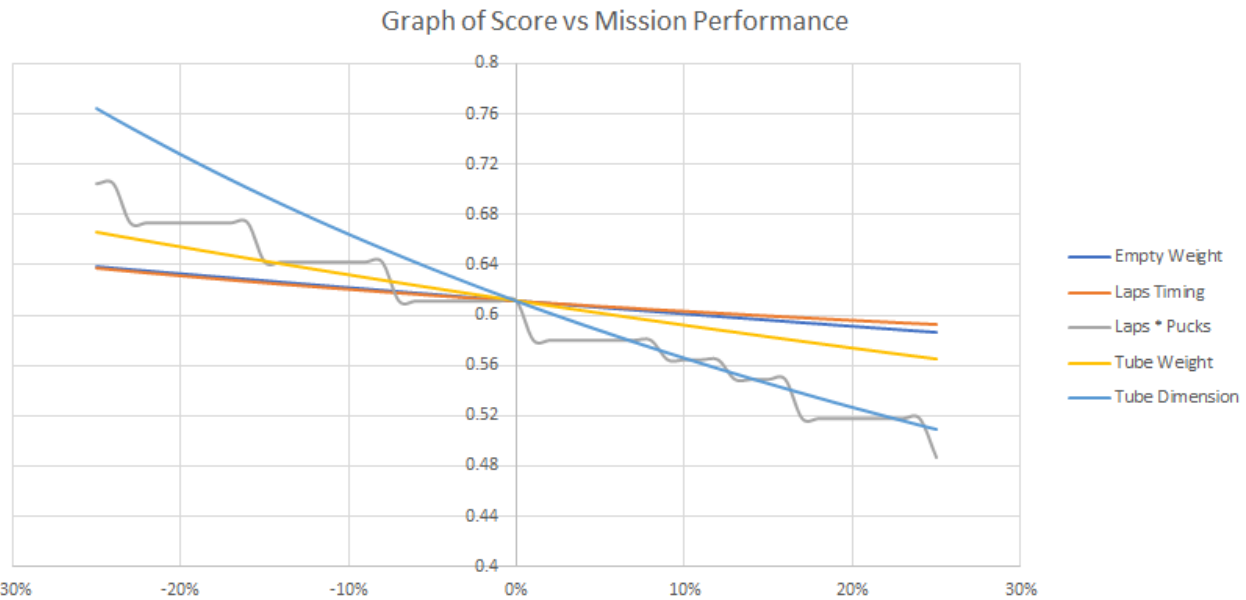


Figure 5: Sensitivity Analysis

The scoring rubrics were analyzed to determine the significance of each parameter on the final score as shown above in Figure 5. We used Microsoft Excel and plotted a graph to visualize the sensitivity of the total score given a change in each parameter. The reference values are estimates of best scores from past year competition as shown in Figure 6 below. (Laps * pucks) for mission 3 score are calculated with a step function.

Parameters	Reference Value	Team Value
Empty Weight	0.8 kg	1.6 kg
Mission 2 Laps Timing	120 s	180 s
Laps * Pucks	25	12
Tube Weight	1.5 kg	3 kg
Tube Dimension (Length + Circumference)	1.785 m	2.224 m

Figure 6: Reference & Team Values

We concluded that the tube-related dimensions such as length and circumference are the most critical parameters. Therefore, we will design our plane with the ability to be compactly stored inside a tube as the leading factor. The next most important parameter is mission 3 score. Due to the discrete nature of the score, it is most efficient to increase the (Laps * Pucks) while staying at the lower boundary of the step function (e.g. aim for 3.2 laps in 5 minutes instead of 3.8 laps). Lap timing in mission 2 is a secondary concern in this year's competition, but it is linked to the (Laps * Pucks) of mission 3. Empty weight is not as crucial this year because the system weight is a summation of the tube and empty weight of the aircraft. Aircraft weight will still be optimized to facilitate launching by hand. Testing and prototyping are required to know what is the critical weight for the plane to be easily hand launched.

3.3. Design Requirements

Based on all the analyses above, we have concluded that the design requirements of our aircraft are as follows:

- Low Take-Off Speed - Since the aircraft will be hand-launched, we need to ensure that our aircraft can reach the take-off speed quickly.
- Large Wing Area - To obtain the high lift necessary for a low take-off speed. The wing area is the most adjustable parameters.
- Small 'Stowed' Cross Section - The size of the tube has the biggest impact on the total score. Therefore, the aircraft should be as compact as possible
- Relatively Low Power Loading - Based on our sensitivity analysis, the plane's speed does not significantly affect the overall score.
- Simple Stowing Mechanism - A simple stowing mechanism is favorable in reducing the system weight to improve the overall score and increase the thrower's ability to hand launch the plane.

3.4. Evaluations of Concepts and Configurations

We have considered several configurations for the aircraft and its components. The weightage assigned to the factors are derived from the analyses above.

3.4.1. Plane Configurations

FOM factors	FOM Values	Monoplane	Biplane	Flying Wing
Compactness	0.35	0	0	-1
Plane weight	0.25	0	-1	1
Ease of manufacture	0.25	1	-1	-1
Lift	0.15	0	1	1
Total	1.00	0.25	-0.35	-0.20

Figure 7: Plane Configurations Figure of Merit

We have determined that compactness is the most critical parameters, followed by both weight and manufacturability. Lastly, we have included total lift into the FOM due to the hand-launch requirements, while excluding drag from the consideration.

Monoplane is the simplest design and has proven countless times that it works well. While the biplane allows a greater wing area to be fitted inside smaller wing span, having wings at the top and the bottom of the fuselage would necessitate a larger tube diameter. Furthermore, if the wingspan or the fuselage's length is less than four times the tube's diameter, it will unnecessarily increase the length of the tube to fulfill the competition criteria of having the tube length four times that of diameter. Moreover, the added

complexity and weight does not justify the previous benefit. In the case of the flying wing, it is the least compact configuration, and require a more complex control mechanism.

3.4.2. Stowing Mechanism Configurations

FOM factors	FOM value	Rotating Wing About Pivot (MV-22B Osprey) 	Folding Wing (Grumman F4F Wildcat) 	Folding wing (Grumman Viking S-3B) 
Compactness	0.50	1	0	-1
Complexity	0.35	1	0	-1
Strength	0.15	0	1	1
Total	1.00	0.85	0.15	-0.7

Figure 8: Stowing Mechanism Configurations Figure of Merit

The compactness of the plane in the stowed position directly affects the required dimension of the tube. As the tube dimensions have the largest influence on our final score based on the sensitivity analysis earlier, the compactness of the plane in the stowed position must be given the greatest weightage. Another important parameter is the complexity of the self-locking mechanism. A simple mechanism is not only light but also significantly simplifies the manufacturing process. Since aligning the wing parallel to the fuselage can minimize the tube diameter and maximize the wing span, rotary wing proved to be the best mechanism for wing storage.

3.4.3. Wing Configurations

FOM factors	FOM value	High 	Middle 	Low 
Ease of manufacture	0.25	1	0	1
Compatibility with stowing mechanism	0.25	1	-1	1
Stress on wing box	0.3	-1	0	1
Stability	0.20	1	0	-1
Total	1.00	0.40	-0.25	0.60

Figure 9: Wing Configurations Figure of Merit

In this section, manufacturability and compatibility with the chosen stowing mechanism are deemed as the deciding factors. Due to the force and stress on the folding mechanism, the low wing configuration is favored over the high wing configuration. The stress on wing box refers to the stress experienced by the structures connecting the fuselage and the wing. This connecting structure will experience large forces during the flight as it transfers the entire lift generated by the wing on to the fuselage. A high wing configuration would experience a tensile force trying to separate the wing from the fuselage during flight while low wing configuration would experience a compressive force that pushes the wing and fuselage together.

3.4.4. Fuselage Configurations

FOM factors	FOM value	Truss	Monocoque	Formers and Stringers
Weight	0.45	1	-1	0
Ease of manufacture	0.35	0	0	1
Ease of repair	0.20	1	0	0
Total	1.00	0.65	-0.45	0.35

Figure 10: Fuselage Configurations Figure of Merit

Weight is regarded as the most crucial aspect of this selection, as the fuselage contributes the most structural weight. Since the driving factor of the tube size is mostly on the wing and tail, we did not include compactness. The fuselage is also the main bulk of the manufacturing process; thus, the ease of manufacture is ranked second next to the weight aspect. Based on the table above, a truss structure is the most weight-efficient structure. Given that an improper landing/takeoff might damage the aircraft, the ease of repair must be taken into account as well. A truss structure is the easiest structure among the three to be fixed quickly.

3.4.5. Empennage Configurations

FOM factors	FOM value	Conventional	Twin-tail	V-tail	T-tail
Ease of manufacture	0.20	1	-1	-1	-1
Stability & Control	0.30	0	0	-1	1
Compactness	0.50	0	1	1	-1
Total	1.00	0.20	0.30	0	-0.40

Figure 11: Empennage Configurations Figure of Merit

In this section, compactness is the primary factor that determines the choice of empennage design as it is one of the driving factor that determines the tube diameter. To avoid further complications, stowing mechanisms in the empennage is to be avoided whenever possible. Stability & control is the next most important factor because without it the aircraft will be difficult to pilot. Therefore, we have selected the twin tail, because the use of other configurations either necessitated massive folding and locking mechanisms for the empennage to fit within the tube, or require a more complicated control scheme involving the merging of control surfaces.

3.4.6. Landing Gear Configurations

FOM factors	FOM value	Tricycle	Tail-Dragger	Bicycle	None
Weight	0.30	-1	0	-1	1
Ease of manufacture	0.20	0	0	-1	1
Ground handling	0.50	1	1	-1	-1
Total	1.00	0.20	0.50	-1	0

Figure 12: Landing Gear Configurations Figure of Merit

Ground handling is taken to be the most crucial factor in the selection of the landing gear because the inability to land without taking significant damage is taken to be a mission failure. The bicycle configuration has poor ground handling; hence it is eliminated. Since the aircraft will be hand-launched, we also considered not putting any landing gear. However, we believe that this will cause the plane to skid on the fuselage during landing and damage the fuselage. A tail-dragger configuration is lighter than a tricycle

configuration as a tail-wheel can be made much smaller than a nose-wheel to create sufficient propeller clearance.

3.4.7. Propeller Configurations

FOM factors	FOM value	Single Pusher	Single Tractor	Multi Tractor
Weight	0.6	1	1	-1
Efficiency	0.4	0	1	-1
Total	1.00	0.4	0.85	-1.00

Figure 13: Configurations Figure of Merit

Single motor configuration is considered to have a relatively better efficiency for small scale model planes. Pusher configuration is less efficient as compared to a tractor configuration of a similar configuration. Single motor planes are preferred over multi-motors since it is heavier and less compact. Lastly, pusher motors pose a safety concern during the hand launch.

3.5. Final Concept

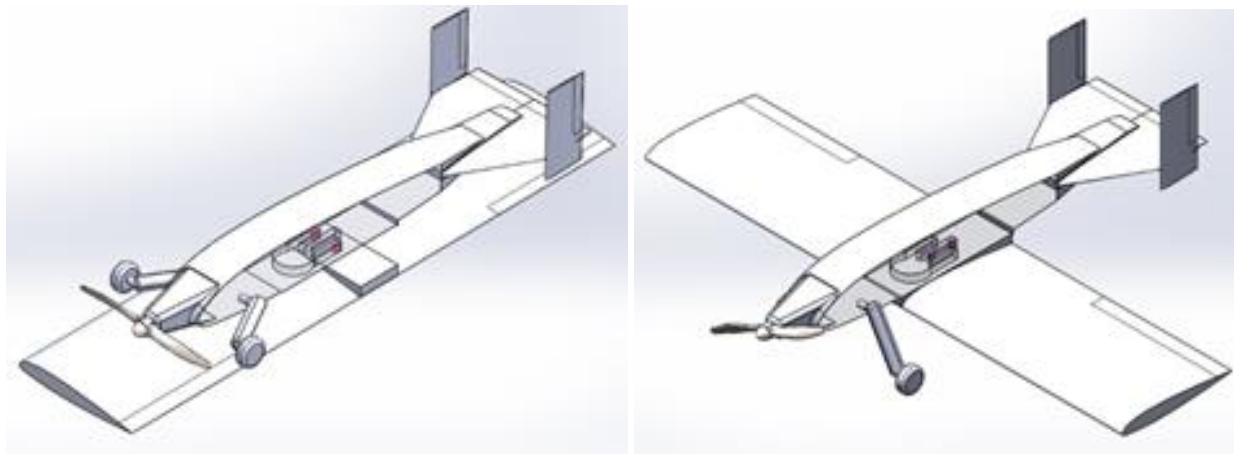


Figure 14: CAD of Conceptual Design

After considering the advantages and disadvantages of the various aircraft configurations, we proceed to select the configurations that are best suited to maximize our competition score. The configurations have been cross-analyzed to ensure that the features complement each other. A concept design has been created as shown in figure 14 above. The elaboration of the final concept is as follows:

Fuselage

The fuselage will be a truss structure, which allows our plane to be lighter while still maintaining good structural strength. Truss structure is easily repaired as the truss members can be easily manufactured and joined.

Empennage

The twin tail configuration was selected because it gives the best compromise between maximizing the wetted area while concurrently keeping the empennage compact enough to fit within the tube. The use of the twin-tail configuration dispenses with the need to fold the empennage to fit it within the tube.

Landing Gear

Although having no landing gears would lead to major reductions in weight and drag, the risk of sustaining damage to mission critical components upon landing is too high. Hence a tail-dragger configuration was selected.

Propeller Configuration

A conventional single tractor configuration was picked. It provides the best compromise between propeller efficiency and weight. A tractor propeller configuration would also facilitate the hand-launching process as it provides a safe clearance of the propeller from the thrower.

Wing

A low wing configuration was chosen despite its poor lateral stability as it scores well in both its compactness and its ability to secure the wing and fuselage together during the flight. Moreover, it synergizes well with our rotating wing mechanism.

Folding Mechanism

A rotary wing configuration is selected as it is the easiest to manufacture and has the best compactness.

4. Preliminary Design

4.1. Design Methodology

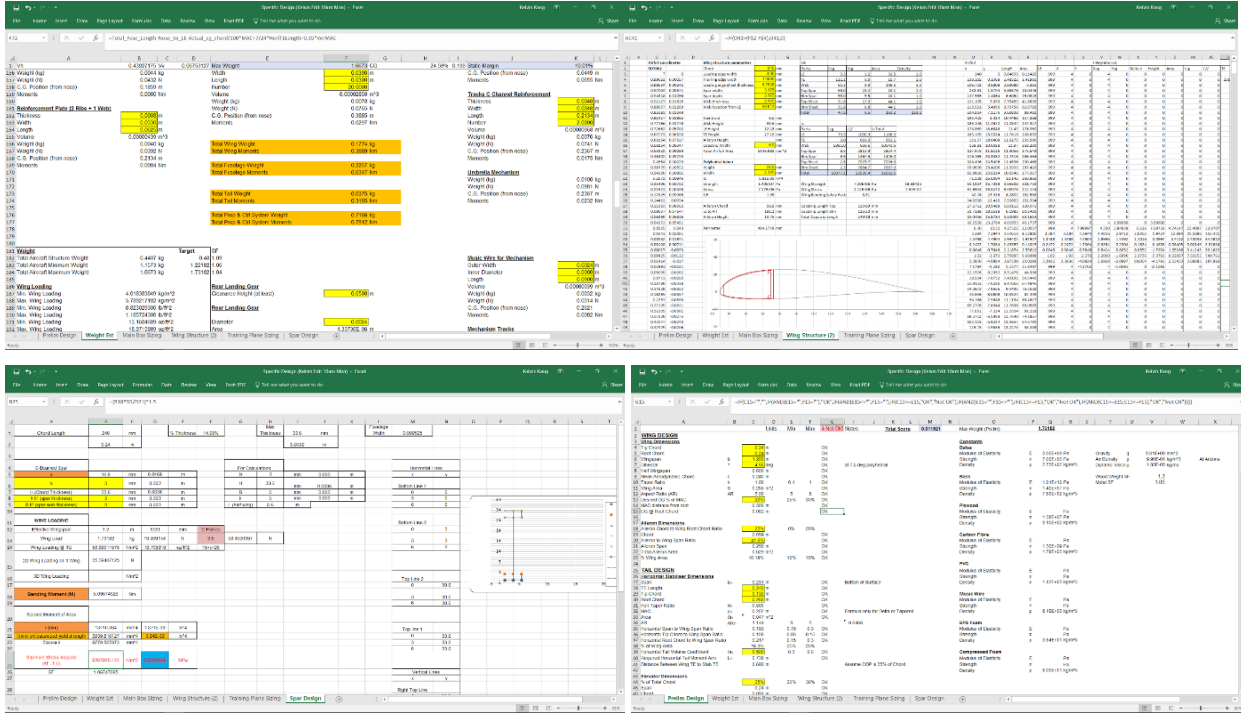


Figure 15: Excel Program for Aircraft Design

We use an iterative approach to tackle our preliminary design. An Excel file (shown in figure 15) containing all the necessary parameters was created to track our plane's sizing and performance parameters (aerodynamics, propulsion, stability, and mission performance). We first include our plane's parameters that we decided on previously based on our sensitivity analysis. These parameters are further refined to give the best competition score through many cycles of manipulating these parameters itself. The steps of iteration are briefly summarized below:

1. Payload Size. We started off by first determining the amount of payload that the aircraft should be carrying. Based on previous year's DBF's winning report data, we make further calculations to estimate the required wing area, structural weight, and the empty weight.
 2. Lift Characteristics. Desired lift characteristics and stall speed, can be obtained with aerodynamic equations using parameters such as the local atmospheric conditions as mentioned in the earlier chapters.
 3. Airfoil Selection. The above-calculated characteristics can be matched to a suitable airfoil that is not only easy to manufacture but also provides the lift characteristics we require.
 4. Drag Characteristics. Lift coefficients obtained in the previous step is then used to find the induced drag, and empirical method is used to find the parasitic drag.

5. Empennage Sizing. As much as possible, we aim to minimize the tail area so that the aircraft can be fitted into a smaller tube. The appropriate parameters including tail volume are then cross-checked to ensure that the tails will still be effective in providing stability despite the small area.

6. Propulsion Characteristics. After meeting the aerodynamic and stability requirements, we then proceed to pick a motor that allows us to fly the aircraft. The power loading is then determined from our mission analysis and the drag polar. The appropriate motor is then selected.

7. Iterate the Process. We then look at the assumptions and estimated sizing we made at the start and change them accordingly to maximize the score until we are satisfied by the parameters in this preliminary design.

The values shown below are the final parameters for our preliminary design after many rounds of iterations.

4.2. Lift Characteristics

4.2.1. Wing Area

Using past DBF competition data, the required wing area and structural weight can be estimated. Based on the sensitivity analysis, we have concluded that we should focus on reducing the plane's size instead of focusing on improving the mission score. Therefore, we will carry the minimum number of 3 pucks as our payload, as we need to make it light enough so that it can be easily thrown.

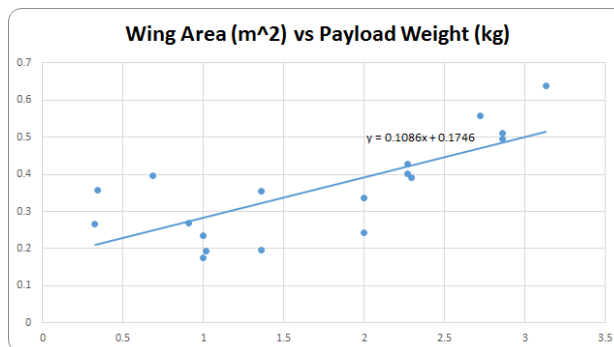


Figure 16: Graph of Wing Area vs. Payload Weight

From the interpolation of the data, we determined that a minimum wing area of 0.23m^2 is needed for an aircraft to carry 510g payload. Due to the hand launch requirements we have decided that we need to provide additional lift. Therefore, we have decided to increase the wing area to 0.288m^2 .

4.2.2. Aircraft Weight

Using similar methods of interpolation from past year's data, we have an estimated structural weight of 0.423 kg, and an empty weight of 0.990 kg. We then added a safety factor of 1.25 to the weight.

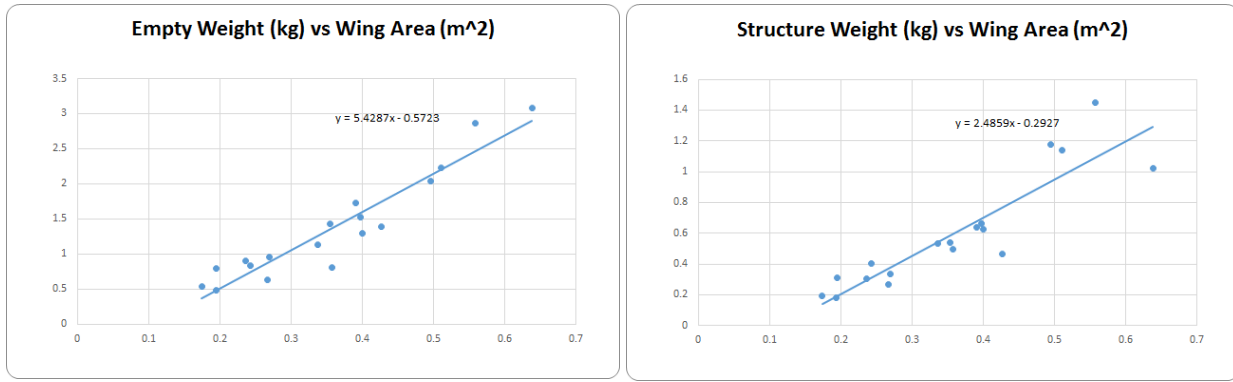


Figure 17: Graph of Structural Weight vs Wing Area

Figure 18: Graph of Empty Weight vs Wing Area

The table below summarizes the estimated weight of our plane based for the preliminary design

	Weight (kg)
Structural Weight	0.528
Empty Weight	1.22
Payload	0.51
Total	1.73

Figure 19: Preliminary Design Weight

4.2.3. Wing Sizing

With the wing area of 0.288 m^2 , there are various wing shapes that we can adopt. From sensitivity analysis, we have concluded that the tube size is the most important parameter. Hence, the focus is to select a wing shape that can fit within the smallest possible tube size.

Limited by design considerations where tube length must be at least 4 times the diameter, we must maximize the space inside the tube through making the stowed plane's length four times the tube's diameter. Therefore, we have decided that the best method that can fit the aircraft into the tube yet maximize the space within is to have a rotational wing with a wing chord that has the same length as the tube's inner diameter. The wingspan will then be limited by the length of the tube. Also, the wing shape would be rectangular without tapering to maximize wing area. Using the wing area required as well as the chord length, we have determined that an aspect ratio to be 4 will best utilize the space inside the tube.

$$AR = \frac{b^2}{S} = \frac{b}{c}$$

However, based on modeling on our preliminary CAD design and the limitation of the rotational mechanism, it is not feasible to place the wing directly at the center of the tube due to axis alignment. Furthermore, the higher AR has been proven to increase the 3D coefficient of lift of the plane as shown by Anderson [1]. Therefore, dimensional changes are made to maximize the use of space within the tube and ensure that the required wing area is met. The sizing of the aircraft wing is as follow:

	Dimension
Chord	240 mm
Span	1200 mm
AR	5
Wing Area	0.288 m ²

Figure 20: Preliminary Design Wing Sizing

Commercial RC aircraft were used to estimate the hand launch speed for a given aircraft size and weight. A safe minimum stall speed of 10m/s is determined from the hand launch test. The experiment will be covered in greater details in the later section.

$$\text{Lift} = \text{Weight} = 0.5 \times \rho \times V_s^2 \times S \times C_{L,\max}$$

$$V_{LOF} = 1.2 * V_s$$

C _{L,max}	Stall speed (V _s)	Take-off speed (V _{LOF})
1.2684	9.693 m/s	11.631 m/s

Figure 21: Preliminary Design Lift Characteristics

During the first iteration, C_{L,max} was assumed to be 1.2. The derivation of the final C_{L,max} will be covered in the later section.

4.2.4. Wing Loading

Another important parameter is the wing loading which reflects the general maneuvering performance of an aircraft. In general, an aircraft with high wing loading has decreased maneuverability as shown by Kermode [3]. As such, we aim to achieve a wing loading that is within the limits of our aircraft structure as well as the motor and battery components.

$$\text{Wing Loading} = \frac{\text{Weight}}{\text{Wing Area}} = 19.71 \text{ oz/ft}^2$$

Aircraft with low wing loading would have more lift and be able to take off and land at a lower speed. Wing loading can affect various other performance parameters such as climb rate, turning and performance and more critically in our case, the stability of the aircraft.

4.3. Airfoil Selection

We gathered airfoils of different series and analyzed their lift and drag characteristics individually. A wide range of airfoil series was selected, such as NACA, EPPLER, Clark, Martin Hepperle and Selig Donovan. Subsonic viscous analysis was done with XFOIL (2-dimensional subsonic isolated airfoil computational software) over a range of α . Lift and drag coefficients were obtained, and drag polars were plotted. The forecasted weather conditions of Tucson provided by Current Results [2] and Engineering Toolbox [4] during the competition period are used to calculate Reynold's number and air density more accurately.

Location	TIMPA Field
Temperature	86 F
Humidity	16 %
Altitude	2185 ft
Barometric Pressure	27.8 Hg
Air Density	0.99 kg/m ³
Air dynamic viscosity	1.85e-5 kg/ms
Estimated Reynold's number	283164

Figure 22: Atmospheric Conditions

Each airfoil is then evaluated individually with the estimated Reynold's number. After iterations and eliminations, we were left with 6 airfoils with desirable airfoil characteristics.

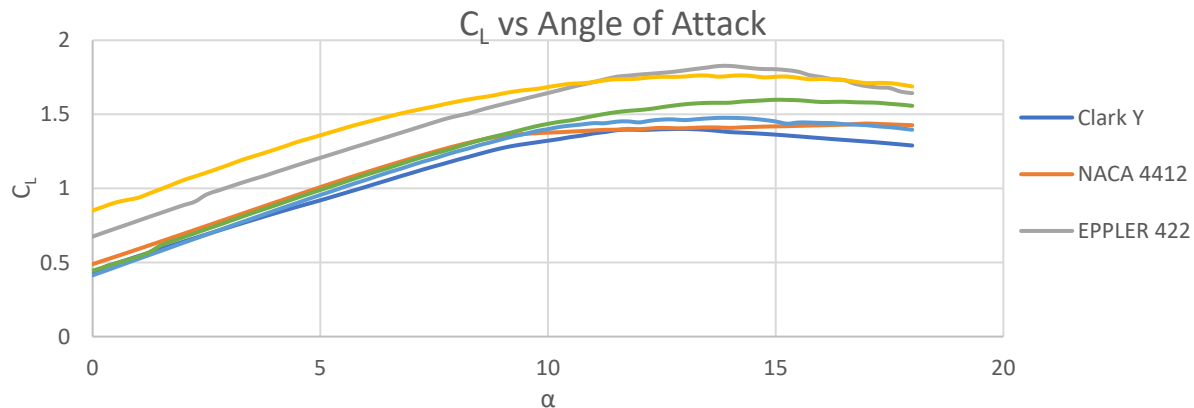


Figure 23: Airfoil C_l vs. Angle of Attack

Airfoil	$C_{L,Max}$	C_{L_0}	$dC_L/d\alpha$	α_{Max}	Airfoil shape
Clark Y	1.4011	0.4195	0.0755	13°	
NACA 4412	1.4381	0.5395	0.0528	17°	
EPPLER 422	1.8266	0.6751	0.08225	14°	
SD7062 (14%)	1.5984	0.4445	0.0769	15°	
MH114	1.7628	0.8508	0.064	14.25°	
SD7034	1.4761	0.4136	0.0758	14°	

Figure 24: Various Airfoil Characteristics

Since the aircraft will be hand launched, it is essential to have a high C_L so that the wing still generates sufficient lift at hand launch speed. EPPLER 422, MH 114 and SD7062(14%) are the top 3 airfoils with maximum C_L across the suitable range of α .

Next, the drag versus lift curve of these airfoils was analyzed.

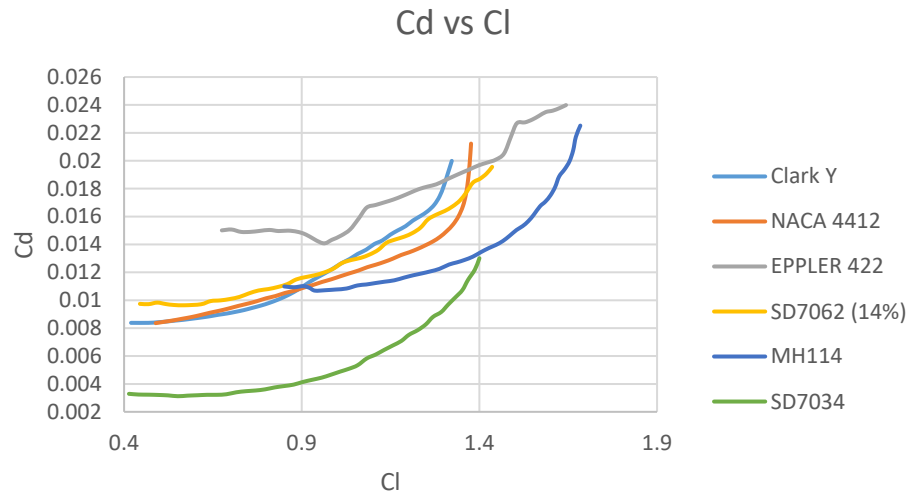


Figure 25: Various Airfoil Drag Polar

The MH114, SD7034 and NACA 4412 are among those with consistently lower drag coefficients. EPPLER 422 is eliminated from consideration due to the extremely high drag coefficient throughout the range of lift coefficients. Although NACA 4412 and SD7034 have low drag coefficients, they were taken out of consideration due to their low maximum C_L .

Sharp trailing edges and highly undercambered airfoils are eliminated because they are hard to manufacture. Despite the precision enabled by our access to laser cutting machines, the balsa wood still splinters easily. Therefore sharp trailing edges are avoided. Highly undercambered airfoils were eliminated as the heat shrink fabrics tend to sag as they have limited surface to attach to, which would result in severe deviation from the intended airfoil. Hence, EPPLER422 and MH114 are removed.

Thus, with considerations on maximum CL, drag, and ease of manufacture, SD7062 is chosen as our designated airfoil. Though slightly undercambered, it has relatively high stall angle of 15 degrees, relatively high maximum lift coefficient, with little drag drawbacks. It has 14% thickness, which made it structurally feasible for our aircraft's small chord length.

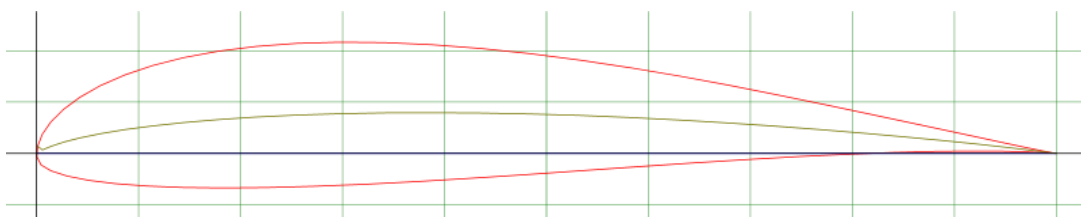


Figure 26: Selected Airfoil Diagram

To account for finite wing conditions, such as the reduced angle of attack due to the downwash caused by the trailing vortices at the wing tip, we will use Prandtl lifting-line theory provided by Anderson [1].

$$\frac{dC_L}{d\alpha}|_{3D} = \frac{dC_L}{d\alpha}|_{2D} \times \frac{AR}{AR + 2} = 0.077$$

Therefore,

$$C_{L,Max} = C_{L,0} + \frac{dC_L}{d\alpha}|_{3D} * \alpha_{max} = 1.268$$

4.4. Drag Characteristics

The wing drag polar can be approximated using the following expression which involves the parasite drag of the wing due to skin friction and pressure distribution around the airfoil as well as the induced drag due to lift. The span efficiency factor is determined using XFLR5 and is estimated to be at a value of 0.85.

$$C_D = C_{D,0} + C_{D,i} = C_{D,0} + \frac{C_L^2}{e(AR)\pi}$$

The aircraft drag polar can be estimated using the same expression with $C_{d,0}$ made up of pressure and skin friction drag from all components including the wing, fuselage, tails, landing gear, etc. $C_{d,0}$ contributions are primarily from skin frictions as the aircraft is designed to minimize flow separation through fairings and tapered aft bodies. Empirical data are used to determine $C_{d,0}$ for the various aircraft parts, parasite drag is calculated at cruise speed which is obtained iteratively to be 26 m/s (See Propulsion Section). The C_d of each component and drag characteristic is as shown below:

	C_d	Percentage
Wing	0.014618	18%
Fuselage	0.004619	6%
Horizontal Tail	0.012748	16%
Vertical Tail	0.01434	18%
Landing Gear	0.003934	5%
Crud Drag	0.014073	18%
Base Drag	0.01269	16%
Induced Drag	0.002238	3%
Overall	0.079262	100%

Figure 27: Drag Build-up Table

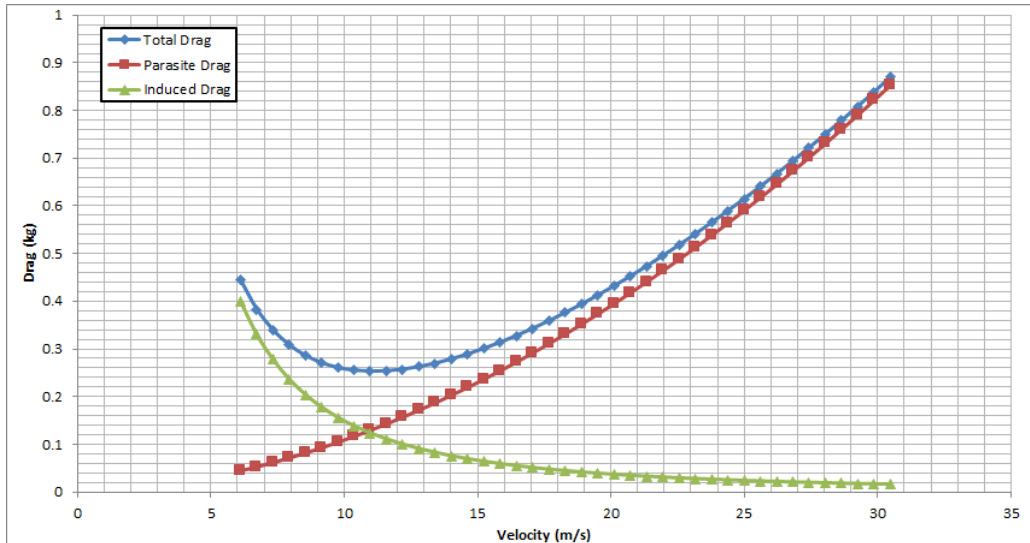


Figure 28: Drag Components

Therefore, our drag polar is:

$$C_D = C_{D,0} + C_{D,i} = C_{D,0} + \frac{C_L^2}{e(AR)\pi} = 0.077 + 0.0748 * C_L^2$$

4.5. Stability & Control

4.5.1. Empennage Sizing & Directional Stability

In our empennage selection, the stability of the aircraft is considered by computing the tail volume coefficients. Structural consideration comes into play here as the moment arm cannot be increased indefinitely. The tube length is fully utilized by making the fuselage length to be close to the tube length, which further reduces the required tail area.

We work backward by first deciding the tail volume coefficient we require, and then finding the required area and moment arm. Since we are using a dual tail, we will include a 'x2' sign for the vertical fin area.

$$V_v = S_h \times \frac{I_h}{S \times c} \quad V_h = S_v \times \frac{I_v}{S \times b}$$

Horizontal Tail Volume Coefficient, V_h	0.44	Vertical Tail Volume Coefficient, V_v	0.0675
Horizontal Tail Moment Arm, I_h	0.65 m	Vertical Tail Moment Arm, I_v	0.695 m
Horizontal Tail Area, S_h	0.0468 m ²	Vertical Tail Area, S_v	0.0168m ² x 2

Figure 29: Preliminary Design Empennage Sizing

We require such a high vertical tail volume coefficient because we will not be installing a rudder. The rudder is not needed because the plane will be hand launched and does not require directional control to taxi on ground. This also removes the complexity in installing rudders on both vertical fin.

Elevator sizing will be based on 25% of the total horizontal stabilizer area.

Elevator	Dimension (m)
Chord	0.051
Span	0.24

Figure 30: Preliminary Design Elevator Sizing

4.5.2. Static Margin & Longitudinal Stability

To calculate static margin, we first estimate the neutral point of the aircraft

$$\frac{x_{np}}{c} = 0.25 \times \frac{1 + \frac{2}{AR}}{1 + \frac{2}{AR_h}} \times \left(1 - \frac{4}{AR + 2}\right) \times V_h = 34.592\%$$

$$\frac{S.M.}{c} = \frac{x_{np}}{c} - \frac{x_{cg}}{c}$$

An ideal range for static margin is from 0.05 to 0.15. However, we wish to keep it at the higher end.

Therefore we will use a static margin of 0.1. Therefore, the desired CG location in terms of chord length is 24.5 %. The final CG location will be determined during the detail design.

4.5.3. Dihedral & Lateral Stability

Previously in conceptual design, we opted for a low wing configuration. The lateral instability of this configuration compels us to consider including a dihedral for additional stability. As such, we need to determine the spiral parameter that would produce a spirally stable aircraft using the following expression:

$$B = \frac{l_v \times Y}{b \times C_L}$$

B > 5, spirally stable B = 5, spirally neutral B < 5, spirally unstable

Via calculations, we have determined that to obtain our desired lateral stability; we would require the dihedral angle to be 4.93 degrees.

Vertical Tail Moment Arm, Iv	0.695 m	C _{L,Max}	1.2684
Effective Dihedral Angle	4.93 deg	B	16.1
Span	1.2 m		

Figure 31: Dihedral Sizing

However, considering that the dihedral wings will interfere with the horizontal body of the fuselage when the wings are rotated into the stowed position, we would have to use tip dihedral i.e. polyhedral. For the effective dihedral angle to be maintained, we require 7.5 degrees of polyhedral angle.

	Root Chord	Tip Chord	Length	Panel Angle from Horizontal	Horizontally Projected Panel Area	Centroid Distance from Root
Mid Section	240 mm	240 mm	350 mm	0	84000 mm	175.00 mm
Polyhedral Section	240 mm	240 mm	250 mm	7.5	59486.7 mm	473.93 mm
			Projected Wing area	286973.4 mm ²	Projected Wing Span	1195.72 mm

Figure 32: Polyhedral Angle Table

$$\text{Effective Dihedral} = \frac{\sum(\text{Horizontal projection} \times \text{Centroid distance} \times \text{Degrees})}{\sum(\text{Horizontal Projection} \times \text{Centroid Distance})} = 4.93^\circ$$

4.5.4. Aileron Sizing

We design our ailerons to be 20% of the total wing area. Since we will be using a polyhedral for our wings, we have decided to have the ailerons throughout the entire span of the polyhedral sections.

Aileron (One Side)	Dimension (m)
Chord	0.06
Span	0.25

Figure 33: Aileron Sizing

4.6. Propulsion Requirements

We use power loading to determine the required power for our plane. As we have determined that the lap timing and speed of the aircraft is not a very critical parameter this year, we decided to use a relatively low power loading for our aircraft. From past experiences and the average power loading of RC planes, we decided to set the required power loading of our plane to be 80 W/lb

	Parameters
Power Loading	80 W/lb
Max Weight	1.73 kg
Power	304.48 W

Figure 34: Power Required

From the nominal power loading, we will then determine the maximum cruise speed.

$$\text{Power Required} = \sqrt{\frac{2 \times W^3}{S \times \rho}} \times \frac{C_D^2}{C_L^3} = \text{Drag} \times V_{cruise,max} = 0.5 \times \rho \times S \times C_D \times V_{cruise,max}^3 = 304.48 \text{ W}$$

$$V_{cruise,max} = 30.1 \text{ m/s}$$

To be conservative, we set the cruise speed to be 26m/s, which gives a power requirement of 198.8 W. This gives us sufficient safety factor and assurance that our plane can hit this speed.

4.6.1. Motor Selection

There are 2 main categories of motors to choose from, brushless and brush motor. In general, brushless motors are more efficient and have longer lifespans as compared to brush motors. Hence, we decided to use a brushless motor. We assume a motor efficiency of 0.8.

Motor	Weight (g)	Nominal Voltage (V)	Nominal Current (A)	Nominal Power (W)
OMA 3825-750	195	14.8	40	473.6
OMA 3815-1000	130	11.1	35	310.8
OMA 3810-1050	102	11.1	30	266.4
OMA 3820-1200	155	11.1	40	355.2

Figure 35: Motor Selection

Therefore, OMA 3815-1000 fulfills our requirement for 80 W/lb power loading.

4.6.2. Thrust Characteristics

Based on manufacturer's specification, the motor can provide a thrust of 1.7 kg for an 11"x7" propeller. Assuming the same motor efficiency of 0.8,

$$T_{av} = 1.7 * 9.81 * 0.8 = 13.3 \text{ N}$$

Moreover, we also use empirical formula to estimate the thrust available

$$\text{Thrust} = ((0.7 \times \text{Motor Power})^2 \times 2 \times \pi \times (\frac{\text{Prop Diameter}}{2})^2 \times \rho)^{\frac{1}{3}} = 14.3 \text{ N}$$

Therefore 13.3 N is a good estimate of the motor thrust.

$$D_{max} = 0.5 \times \rho \times S \times C_D, max \times V_{cruise}^2 = 7.65 \text{ N}$$

Hence, the motor provides sufficient thrust to overcome the drag force

4.7. Mission Models

The flight mission can be divided into several portions: take-off, climb, cruise, turn and descent. We will be using standard aircraft performance parameters to model these manoeuvres while altering some assumptions to fit it for this year's mission requirements (e.g. hand launch).

4.7.1. Takeoff & Climb Performance

Since the plane will be hand launched, conventional take off performance such as Takeoff Field Length and Lift-off Distance are not applicable. We will be analyzing the takeoff and climb performance together as they are linked for hand launches. A small α is assumed for take-off, climb and descent calculations.

From our testing data, we determined that the hand launch velocity of our plane to be 9 m/s (see 'Testing Section')

We will use the lift produced, gravity acceleration, and height of throw from the ground to estimate the time required for the plane to fall to the ground.

Launch Velocity	9 m/s	Cl Max	1.2684	Lift	11.476 N
Max Weight	16.989 N	Drop Rate	3.2 m/s	Height	1.9 m
Drag	2.3 N	Thrust	13.3 N	Forward Acceleration	8.3 m/s
Time to Fall	1.1 s			Time to reach V _{LOF}	0.3s

Figure 36: Takeoff Performance

Therefore, our plane has sufficient lift and thrust for hand launch.

4.7.2. Straight Level Flight Performance

We will assume constant cruise speed of 26 m/s during straight level flight.

4.7.3. Turning Performance

Steady coordinated turn is assumed for turning performance. Therefore, the bank angle on the aircraft is solely based on the load factor n.

$$n = \frac{L}{W} = \frac{1}{\cos(\theta)}$$

Our plane is designed to handle at least 2.5 G of load.

$$\text{banking angle, } \theta \cos^{-1}(1/2.5) = 66^\circ$$

$$\text{Turning Stall Speed} = V_s * \sqrt{n} = 15.3 \text{ ms}^{-1}$$

$$\text{banking radius} = \frac{V^2}{\tan(\theta) \times g}$$

$$\text{Time taken to turn} = \pi \times \frac{\text{Banking Radius}}{\text{Banking Speed}} = \frac{V \times \pi}{\tan(\theta) \times g}$$

Therefore, the time taken for the plane to complete the turn is inversely proportional to the banking speed. However, it is dangerous to fly near the stall speed and it will be inefficient to decelerate and accelerate the plane many times. Hence, we have decided to bank at 21 m/s

4.7.4. Descent Performance

The time taken to land is not included inside the allocated 5 mins of mission time. Therefore, we have decided to add an additional 30 secs endurance for landing approach. This estimate is derived based on experience from the previous team.

4.7.5. Capabilities & Uncertainties

Since our model uses aircraft performance estimates that are used in commercial airplanes, we can be certain of its accuracy. However, we will still include a factor of safety; this is because there are areas of uncertainties which we cannot estimate, such as the interference drag of our plane, the actual air density at Tuscon and the wind conditions during the competition.

4.8. Estimated Mission Performance

In all the missions, we set aside 20 secs for takeoff.

4.8.1. Rated Aircraft Cost Estimate

Empty Weight	2.69 lb	Tube Circumference	38.34 in
Tube Weight	6.39 lb	Tube Length	49.2 in
RAC	795.289		

Figure 37: Preliminary Design RAC

4.8.2. Mission 1 Performance

We will fly our aircraft without payload for 3 laps. Based on this estimate we will achieve a score of 1 for M1.

	Distance (m)	Time Taken (s)	Battery Consumed (mAh)
Steady Flight	152.4	5.389	35.38
180 deg turn	61.6	2.935	6.96
Per Lap	856.147	34.0	169.38
Total Mission	2568.44	119.889	508.14

Figure 38: Preliminary Design M1 Performance

4.8.3. Mission 2 Performance

We will fly with a payload of 3 pucks for 3 laps. Based on this estimate we will achieve a score of 1.99 for M2.

	Distance (m)	Time Taken (s)	Battery Consumed (mAh)
Steady Flight	152.4	5.389	35.38
180 deg turn	61.6	2.935	6.96
Per Lap	856.147	34.0	169.38
Total Mission	2568.44	119.889	508.14

Figure 39: Preliminary Design M2 Performance

4.8.4. Mission 3 Performance

We will fly with a payload of 3 pucks for 8 laps. Based on this estimate we will achieve a score of 5.84 for M3.

	Distance (m)	Time Taken (s)	Battery Consumed (mAh)
Steady Flight	152.4	5.389	35.38
180 deg turn	61.6	2.935	6.96
Per Lap	856.147	34.0	169.38
Total Mission	6849	255.9	1355

Figure 40: Preliminary Design M3 Performance

5. Detail Design

5.1. Final Design Parameters

Wing		Aileron (One Side)		Fuselage	
Span	1.2 m	Span	0.25 m	Length	0.777 m
MAC	0.24 m	MAC	0.059	Width	0.09 m
Aspect Ratio	5	Deflection	20 deg up 15 deg down	Height	0.11 m
Wing area	0.288	Elevator		Electrical Systems	
Airfoil	SD7062(14%)	Span	0.24 m	ESC	Tahmazo Pro-C A-40
Static margin	9.9%	MAC	0.051 m	Radio receiver	Spektrum AR6260
		Deflection	± 15 deg	No. of servos	3

Vertical stabilizer (Both Side)		Horizontal Stabilizer	
Airfoil	Flat plate	Airfoil	Flat plate
Effective span	0.154 m	Effective span	0.231 m
Effective tip chord	0.174 m	MAC	0.202 m
Effective root chord	0.085 m	Area	0.047m ²
Area	0.0337 m ²		

Batteries		Motor	
Type	Elite NiMH	Type	OS motor OMA 3815-1000
Capacity	2100 mAh	KV	1000
I_max	31.5 A	Rated voltage	11.1V
Nominal V	13.2 V	Rated current	35A
Number of cells	11	Maximum current (5 s)	60A

Figure 41: Final Design Parameters

5.2. Structural Characteristics

The aircraft is designed to withstand loads that are higher than loads experienced during normal flight. As the aircraft is designed with landing skids instead of a regular landing gear, landing on the rough tarmac is expected to produce a violent deceleration. From the frame-by-frame analysis of our flight trial video with our prototype, the complete deceleration of our plane occurred within 0.2 secs after landing. This landing deceleration was calculated to be more than 5Gs. The aircraft structure must be able to withstand such loads without failing.

5.2.1. Fuselage Design

The fuselage comprises of three parts: the nose, the main body, and the tail. The nose contains the motor mount and is tapered for better aerodynamics. The nose cavity also contains part of the main battery pack to keep the CG forward. The main body has a hatch that encompasses the top front half of the fuselage to facilitate loading of the payload and electronics. The cargo bay is located at the front half of the main body. The internal tail structure is empty save for the wiring that connects to the elevator servo. It is tapered to expose the horizontal and vertical stabilizers to clean airflow.

½" balsa bulkheads connect the three parts to one another. The bulkheads are created by gluing four pieces of 1/32" balsa sheets such that their grains alternate between vertical and horizontal directions, giving strength in two dimensions. The bulkheads are designed to have Jigsaw features at the bottom where it joins to the mechanism tracks to assist in alignment and increasing gluing surface.

The structure consists of longerons at each corner and a traditional Warren truss on each side, which provides high strength while keeping material weight low.

The electronics and payload in the cargo bay are attached to the cargo floor with velcro. Heavier components such as the main battery and the payload of pucks are additionally secured with velcro straps that run under the cargo floor and press the components tightly into the cargo floor to prevent the components from shifting in flight.

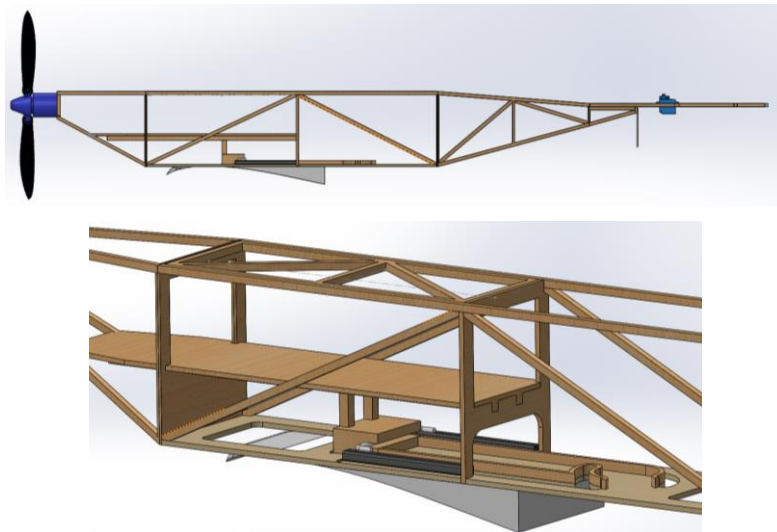


Figure 42: Fuselage Truss Design

5.2.2. Wing Design

The main wings are constructed with a main span that runs under the fuselage and a 7.5 deg polyhedral at each end of the main span. The parts are made using the traditional ribs and spars method. All the ribs are made of balsa. The middle two ribs are 3/16" thick, the ribs at the junction where the polyhedral meets the main span are 1/8" mm thick. The remaining ribs are 1/16" thick. Balsa spars run across the ribs, one each on the top and the bottom. Shear webs made from 1/16" balsa are glued onto the spars, between the ribs. They help the wing resist bending loads by keeping the spars at the proper distance from each other. A strip of 1/32" balsa is glued across the trailing ends of the ribs on the main span. The trailing edge of the balsa strip is sanded down to from a sharp trailing edge to the airfoil, minimising airflow separation. The polyhedrals are constructed in a similar fashion, with exception to the trailing edges. The trailing edges of the polyhedrals are truncated with a strip of 1/32" balsa that spans each polyhedral.

The ailerons span the entire span of the polyhedrals. They are constructed with ribs formed from the trailing edges of the airfoil and covered with 1/32" balsa sheets. The ailerons are attached to the main wings using fiberglass reinforced tape along the upper surfaces.

The top and bottom leading edges of the main span and polyhedrals are covered in 1/32" balsa sheets to form a stiff D-box that increases rigidity against bending and torsional loads. Calculations show that with the D-box, bending stresses on the wing is 40% lower. The main span, polyhedrals and ailerons are sheeted with Monokote to form an unbroken surface.

Two carbon fiber tubes are glued with epoxy at the two middle thick ribs to connect our wings to the fuselage. A 2.3mm music wire is then tied to the tubes to prevent it from falling off from the fuselage.

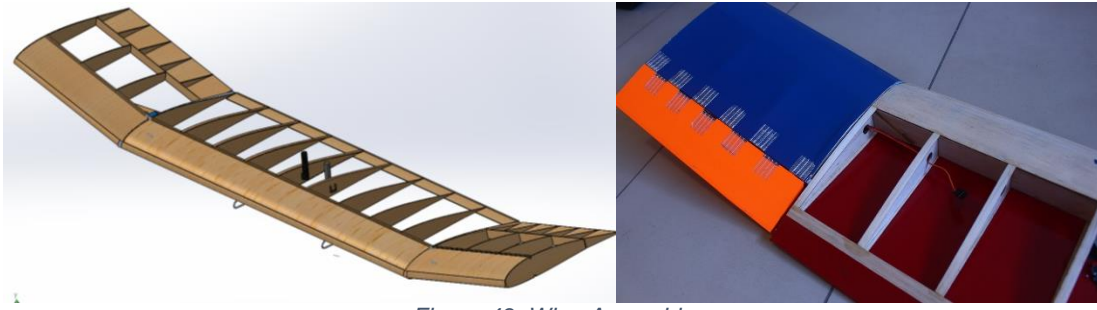


Figure 43: Wing Assembly

5.2.3. Mechanism Tracks Design

The tracks of the mechanism are constructed out of a single piece of basswood. This basswood is integrated into the bottom of the main body fuselage to provide additional strength and rigidity to the structure. Holes are cut into the piece to lighten it. Two narrow tracks are cut on the basswood as guiding rails for the movement of the carbon fiber tube between the plane's in flight and stowed condition. This carbon fiber tube connects the fuselage to the wing as it is glued to the middle two wing ribs. The two carbon fiber tubes have to be at the center of the fuselage in the longitudinal direction to minimize the cross section of the stowed configurations. On the other hand, the wing needs to be closer to the wing during the flight to achieve the required CG location. Hence, a long track is needed.



Figure 44: Plan View of Mechanism Tracks

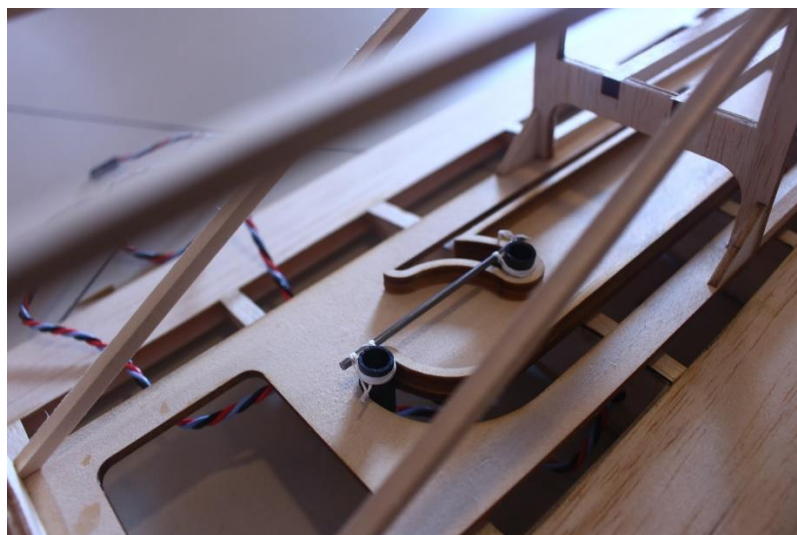


Figure 45: Carbon Fiber Tubes Resting on the Tracks

5.2.4. Locking Mechanism

The locking mechanism is situated to keep the wing securely in place for in-flight condition. Our locking mechanism is sourced from conventional foldable umbrellas. The locking structure is sawed off from an umbrella and placed on the basswood tracks. The umbrella locks keep the wing in place by preventing horizontal movement of the carbon fibre tube. Strings are added to make the umbrella lock accessible from outside the fuselage. The strings enable us to unlock the mechanism to move the wings back into its stowed position.

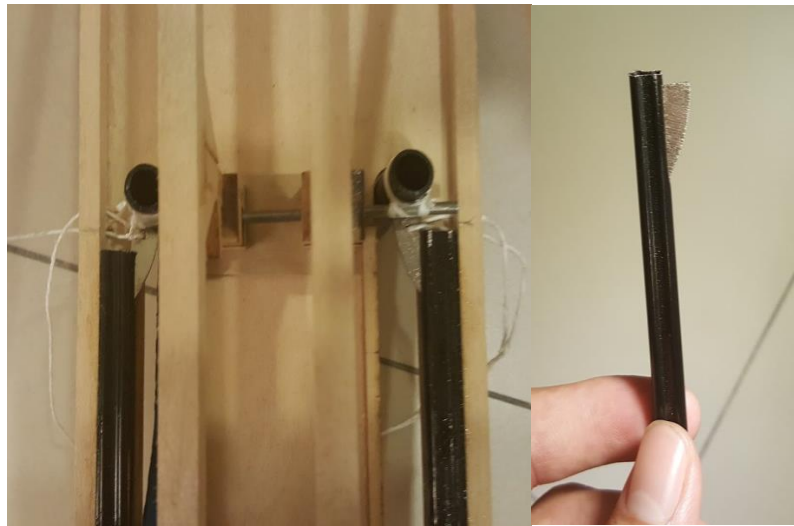


Figure 46: Locking Mechanism

5.2.5. Empennage Design

The horizontal stabilizer is a flat plate. It is formed by a frame of 3/16" balsa trusses which are then sheeted with Monokote. Two slots are provided for in the frame for the vertical stabilizers to slot into. As there are no rudders, each of the two vertical stabilizers is cut from a piece of 5.2 mm foam. The vertical stabilizers are glued into place in the slots.

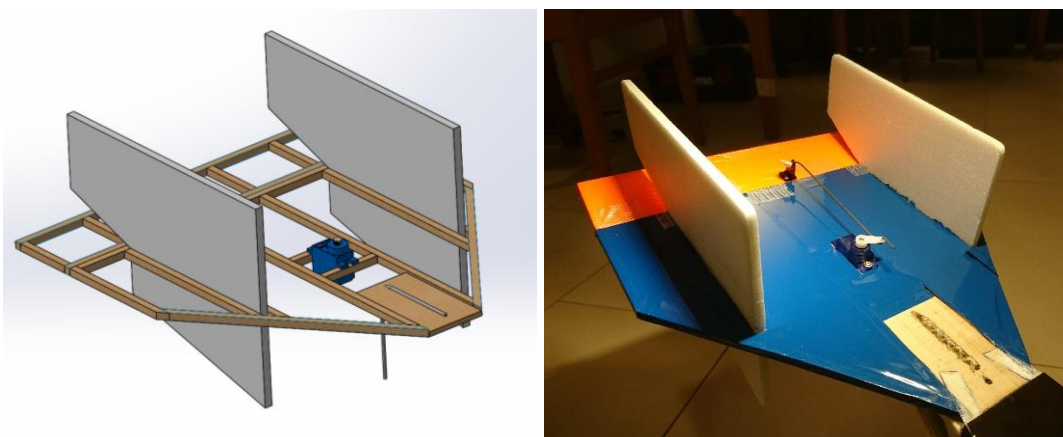


Figure 47: Empennage Assembly

5.2.6. Landing Gear Design

Since no takeoff run is required of the aircraft, we decided to forgo wheeled landing gears in preference for a lighter configuration of landing skids. The landing skids are made from bent segments of 2.3 mm thick music wire. Music wire is chosen as it is durable and resistant to abrasion. Music wire can also deform elastically during the violent forces experienced upon landing, helping to cushion the impact. The two landing skids in the main wings are tied to the shear webs in the wing with dental floss and reinforced with epoxy. The webs are further reinforced with a 1/32" sheet of plywood. For the tail skid, a similar method of attachment is employed in attaching the skid to a 1/8" piece of balsa located on the horizontal stabilizer.

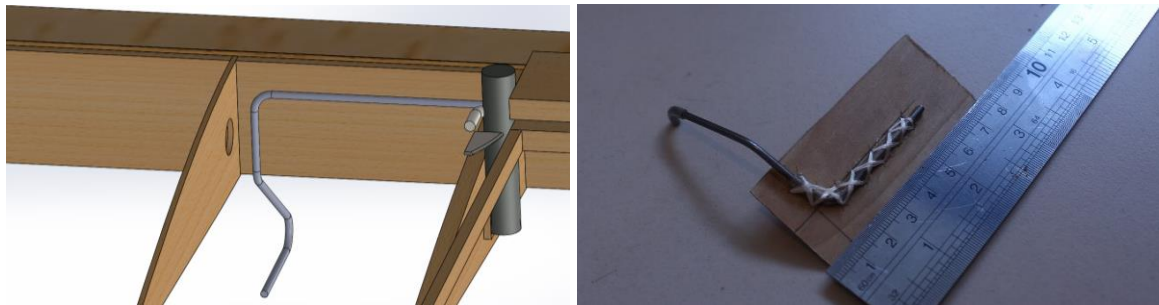


Figure 48: Landing Skid Assembly

5.2.7. Tube Design

The tube comprises two main components: the outer shell and covers which give the tube its shape, and the dunnage to secure the aircraft. The tube and covers are made from 1 cm thick Expanded Polystyrene Styrofoam (EPS). The dunnage is made of many strips of styrofoam 5 cm thick cut to different lengths and glued together; this creates a cradle of styrofoam 'cilium' that follows the contours of the airplane. A unique cradle is separately created for the top and bottom halves of the aircraft. The two cradles are put together with the aircraft nested in between to form a cylinder that is then fitted into the outer thin tube. The caps are attached to the ends of the tube with velcro.

5.3. Propulsion System

5.3.1. Propeller Selection

Since we will be using foldable propellers to ensure that it can be fitted inside the tube, the ground clearance is the main limiting factor of the propeller size available from the airplane when it is horizontal. The size of the propeller used is determined to be 11"x8" from the motor test, which is documented later in the report.

5.3.2. Main Battery Selection

In the competition, there are only 2 allowable types of batteries, NiMH or NiCd. We decided to go with NiMH as it has better energy capacity as compared to NiCd. Also, NiCd has problems of memory effect. Thus it has to be fully discharged before recharging each time. Both types of batteries have similar energy densities. However NiMH has greater performance in high-drain applications i.e. higher power density.

Based on the motor propeller configuration mentioned above, about 12.6V is required to power the motor, hence the combination of battery used has to be able to provide that amount of power.

Battery	Capacity (mAh)	Voltage per Cell (V)	Max Discharge(A)	Weight per cell (g)	Estimated Score
Saft VH Cs 3200 XL	3000	1.2	40	58.0	0.0085
Elite 2100	2100	1.2	30	32.6	0.0087
Elite 1500	1500	1.2	16	22.97	0.0085

Figure 49: Battery Selection

From the estimated scores, Elite 2100 gives the best performance. Since the motor requires 12.6 V, we have chosen 11 cell battery arrangement to provide a nominal voltage of 13.2 V. Taking into consideration that the longest possible flight duration is 5 minutes and additional safety factor, the battery should last 6 minutes. Therefore, with 2100mAh, the average ampere the battery should be discharging is:

$$\text{Current, } I = \frac{\text{Capacity}}{\text{Time}} = \frac{2100}{1000} * \frac{60}{6} = 21 \text{ A}$$

The maximum discharge of 30A is also useful to give the airplane the extra power required during takeoff.

5.3.3. Control System Selection

For the servo selection, the deciding factors are the servo's weight and its ability to generate sufficient torque. Typically, servos with plastic gears are used as they are lightweight and are still capable of providing the necessary torque for an RC model airplane. The conventional servo used for RC models weigh about 9 grams and are known to provide sufficient torque.

Servo Model	Weight (grams)	Torque (kg/cm)
Futuba S3117	9	1.7
Futuba S3156	9.3	2.4
Nitec HS-5055MG	9.5	1.6

Figure 50: Servo Selection

Futuba S3156 is the selected servo as at a weight of 9.3g; it can provide a torque of 2.4 kg/cm which is slightly above what is required.

5.3.4. Power Estimate

Based on the battery selection data, the estimate for the motor power is then fine-tuned.

$$\text{Nominal Power Loading} = \text{Voltage} \times \text{Nominal Current} \times \text{Motor Efficiency} = 221 \text{ W}$$

$$\text{Burst Power} = \text{Voltage} \times \text{Nominal Current} \times \text{Motor Efficiency} = 316 \text{ W}$$

$$\text{Nominal Power Laoding} = 58 \text{ Wlb}^{-1}$$

$$\text{Maximum Power Loading} = 82 \text{ Wlb}^{-1}$$

5.4. Weight & Balance

An excel that tracked every single component of the aircraft was created to estimate the weight and moment arm from the nose to find the center of gravity of the aircraft.

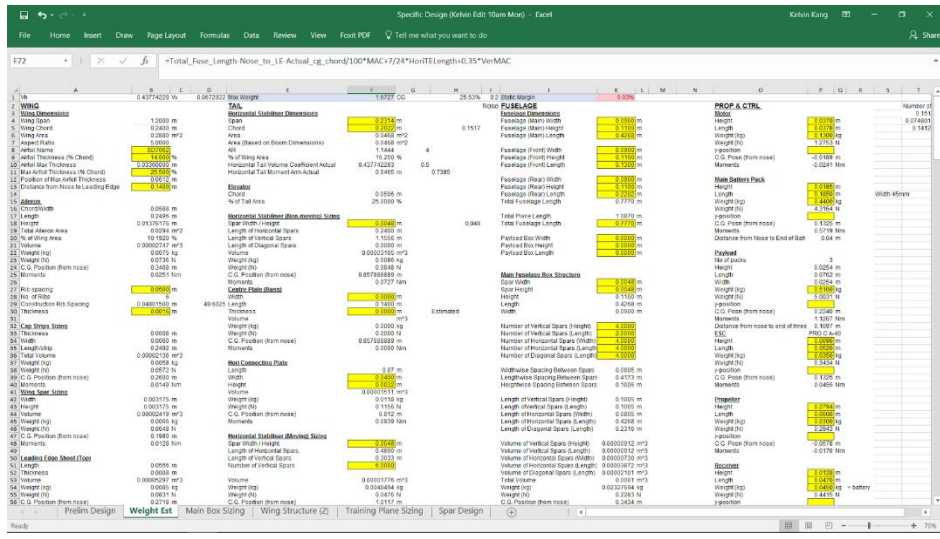


Figure 51: Excel Programming for CG Estimate

5.4.1. Mission 1

Total Wing Weight	0.1774 kg	Total Tail Weight	0.0430 kg
Total Wing Moments	0.3889 Nm	Total Tail Moments	0.3672 Nm
Total Fuselage Weight	0.2257 kg	Total Prop & Ctrl System Weight	0.7166 kg
Total Fuselage Moments	0.6347 Nm	Total Prop & Ctrl System Moments	0.8844 Nm
Total Weight			1.1627 kg
CG (% of Chord)			24.78%

Figure 52: Mission 1 CG Estimate

5.4.2. Mission 2 & 3

Total Wing Weight	0.1774 kg	Total Tail Weight	0.0430 kg
Total Wing Moments	0.3889 Nm	Total Tail Moments	0.3672 Nm
Total Fuselage Weight	0.2257 kg	Total Prop & Ctrl System Weight	0.7166 kg
Total Fuselage Moments	0.6347 Nm	Total Prop & Ctrl System Moments	0.7912 Nm
Total Payload Weight	0.51 kg	Total Weight	
Total Payload Moment	1.1207 Nm	CG (% of Chord)	

Figure 53: Mission 2 & 3 CG Estimate

The CG estimate above shows that the battery needed to be shifted in position between the two configurations. The CG of the aircraft will change slightly, but the static margin will remain fairly constant at around 10%

5.5. Rated Aircraft Cost

After further iteration on our design, the updated RAC are as follows:

Empty Weight	2.563 lb	Tube Circumference	38.34 in
Tube Weight	6.39 lb	Tube Length	49.2 in
RAC	783.85		

Figure 54: Detail Design RAC

5.6. Computational Fluid Dynamics

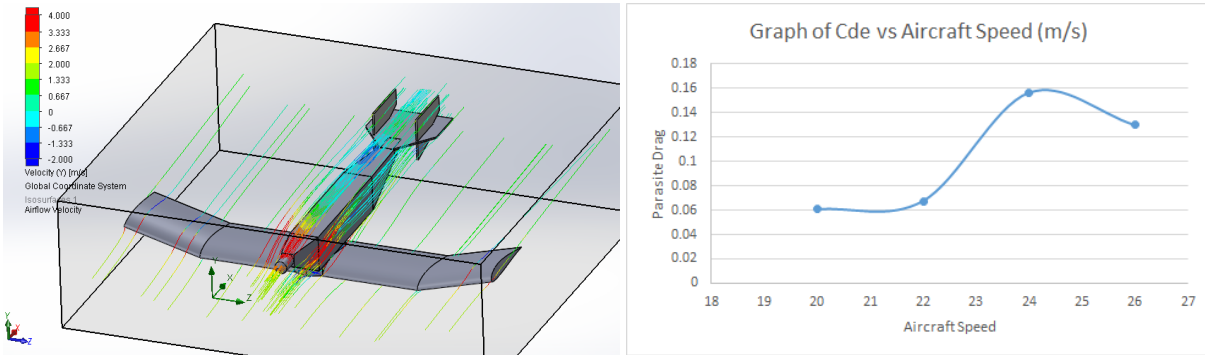


Figure 55: CFD Analysis Results

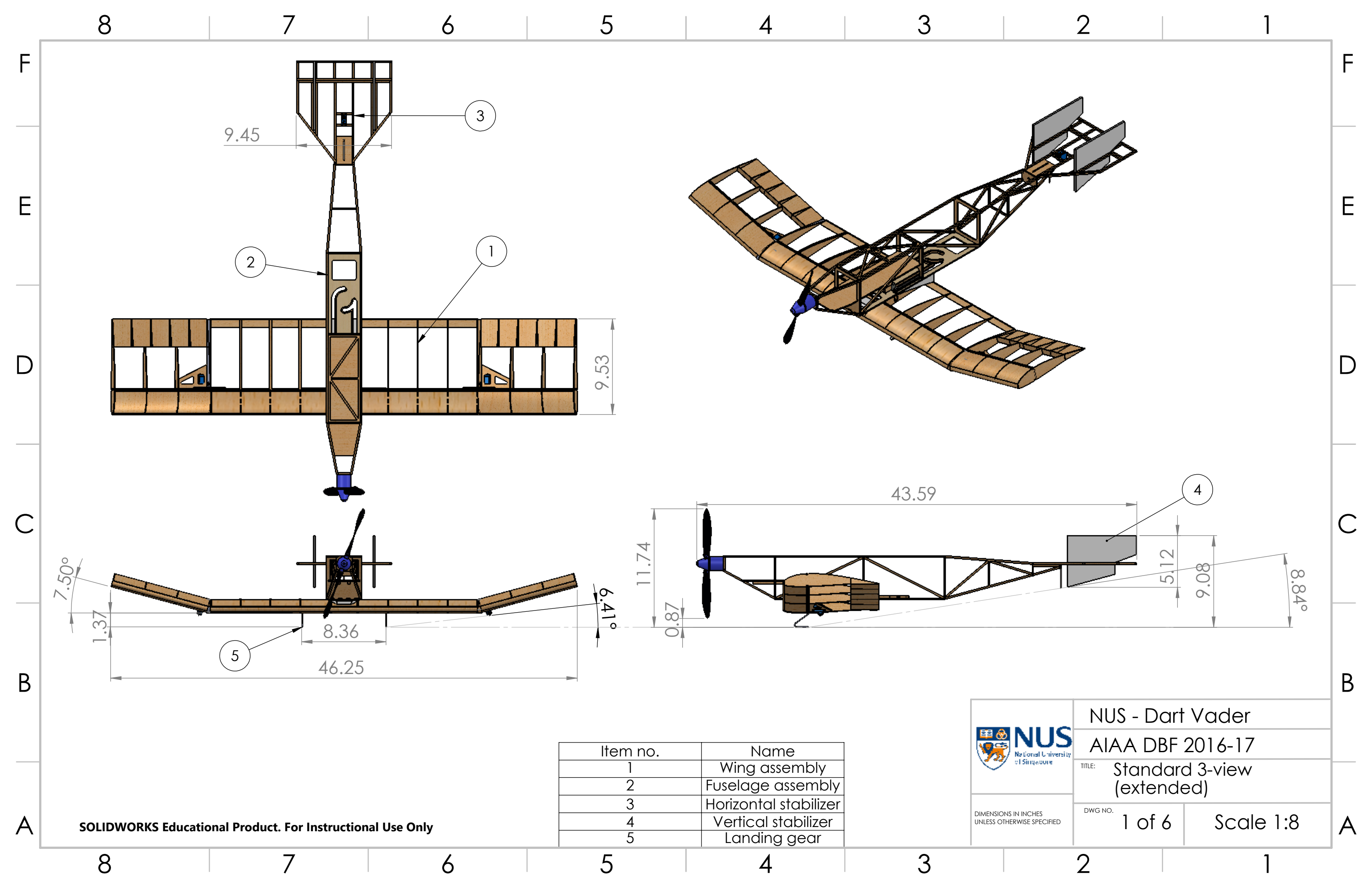
After we had finalized our detail design, we ran our model on a Computational Fluid Dynamics software to estimate the drag force on our airplane. We realize that up to 22m/s our parasite drag is close to our preliminary design values. However, from 24 m/s onwards there is a jump in the parasite drag values. Further analysis of the streamline and flow speed reveals that at 24m/s the flow separation significantly increases. Therefore, this limits our maximum speed of our airplane to 22m/s

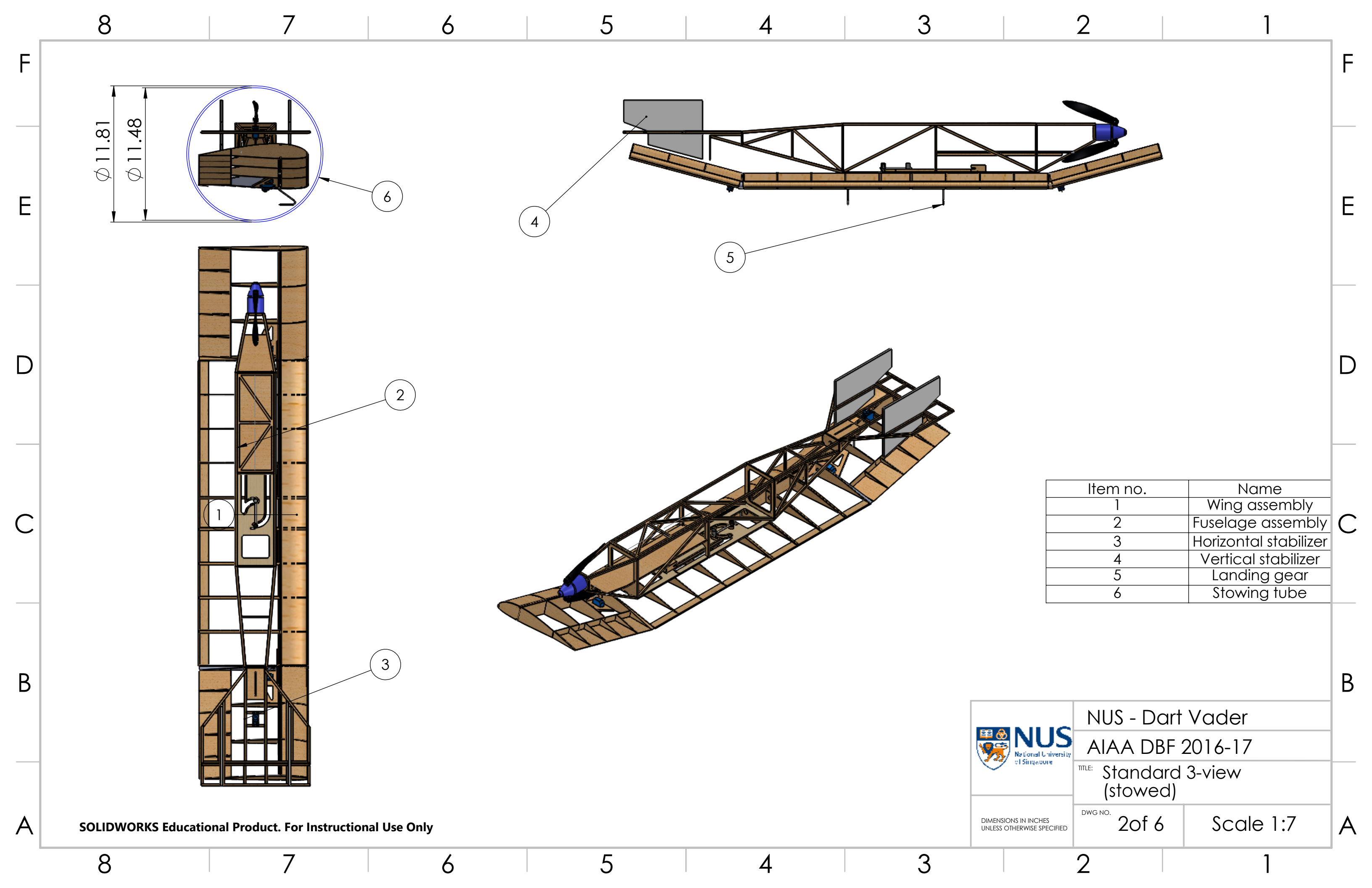
5.7. Performance Characteristics of Final Design

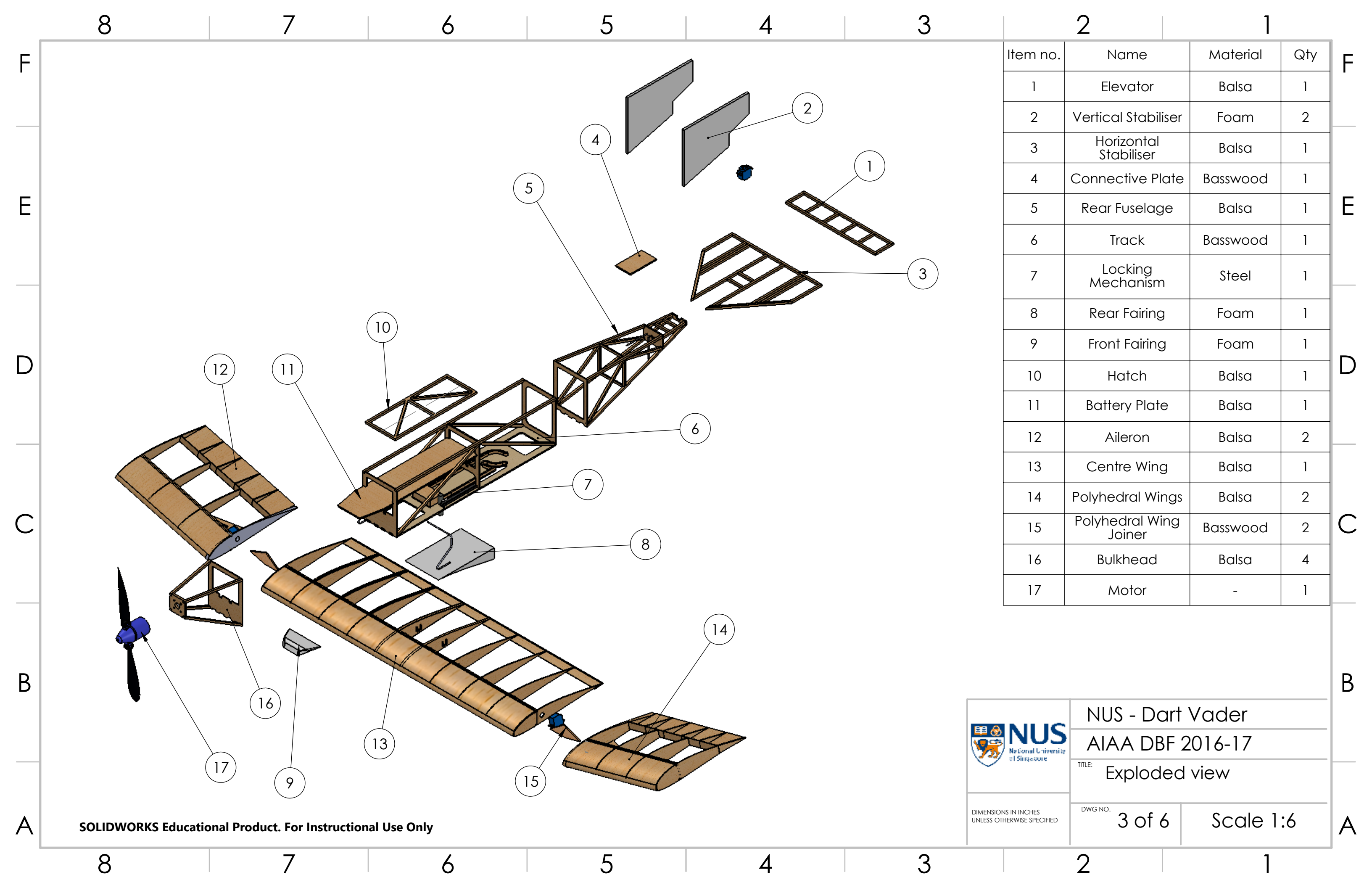
	Laps	Time Taken (s)	Score
Mission 1	3	138.3	1
Mission 2	3	138.3	1.734
Mission 3	6	256.7	4.88

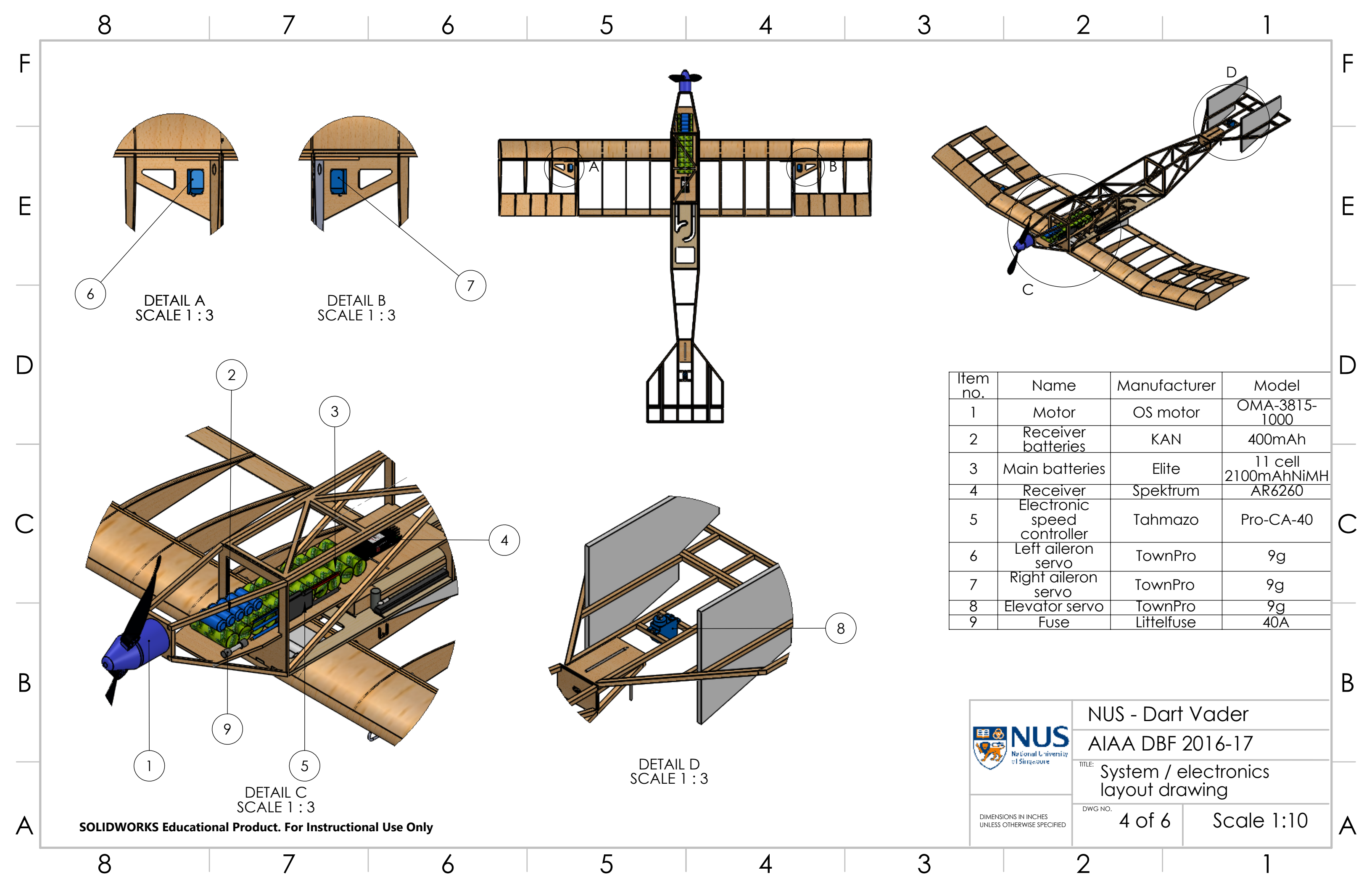
Figure 56: Detail Design Mission Performance

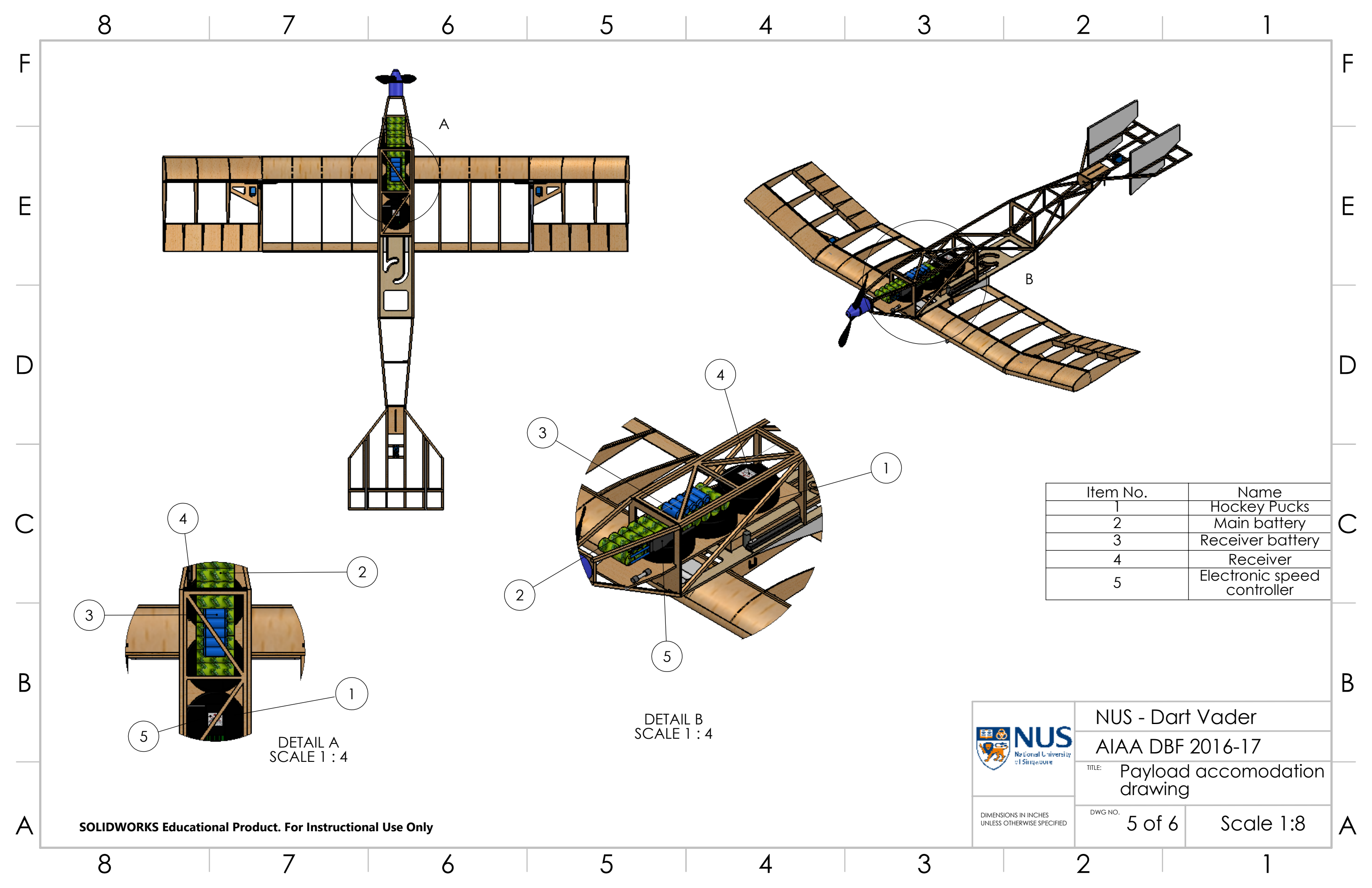
5.8. Schematic Drawings

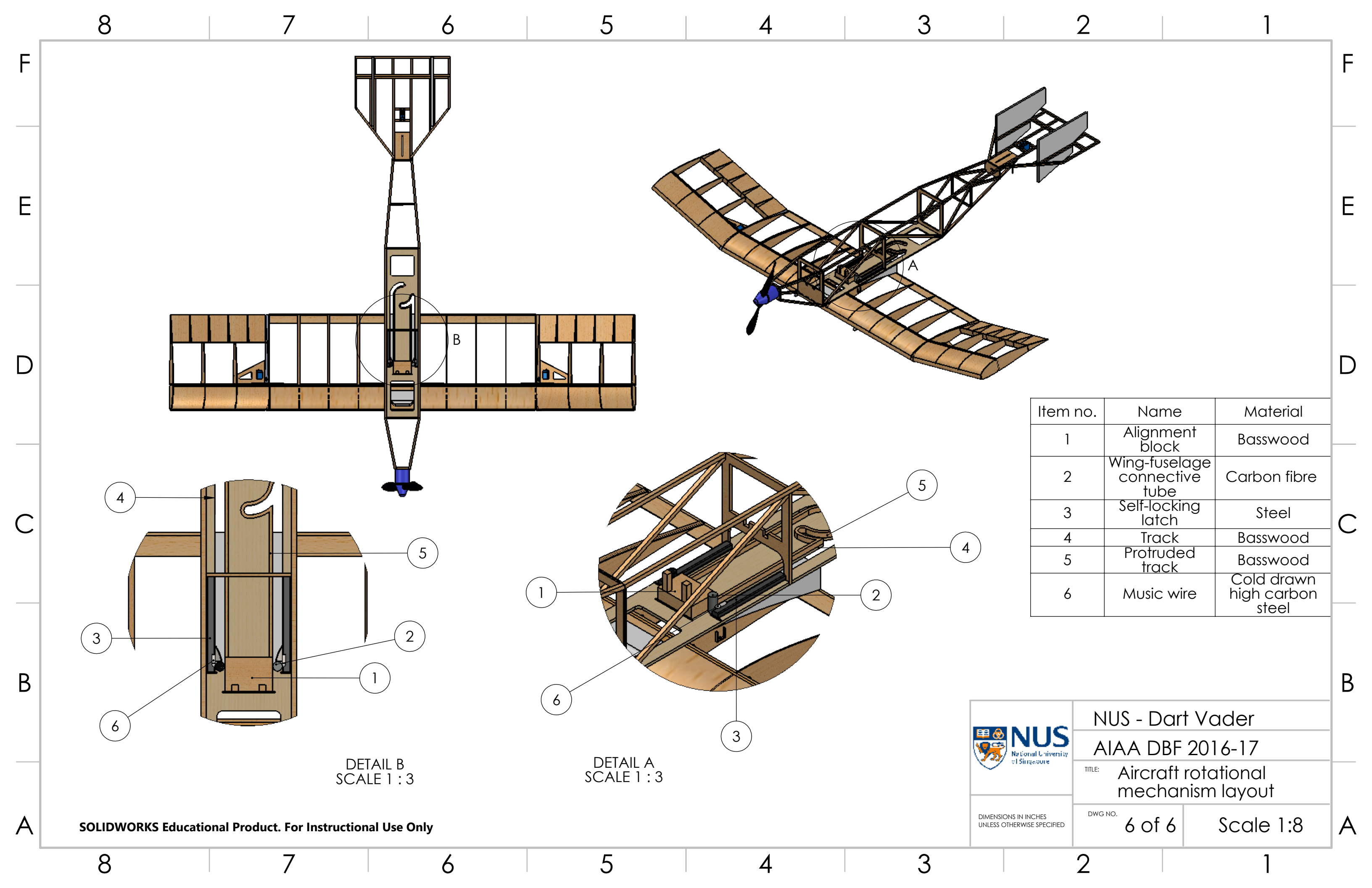












6. Manufacturing Plans

6.1. Milestone Chart

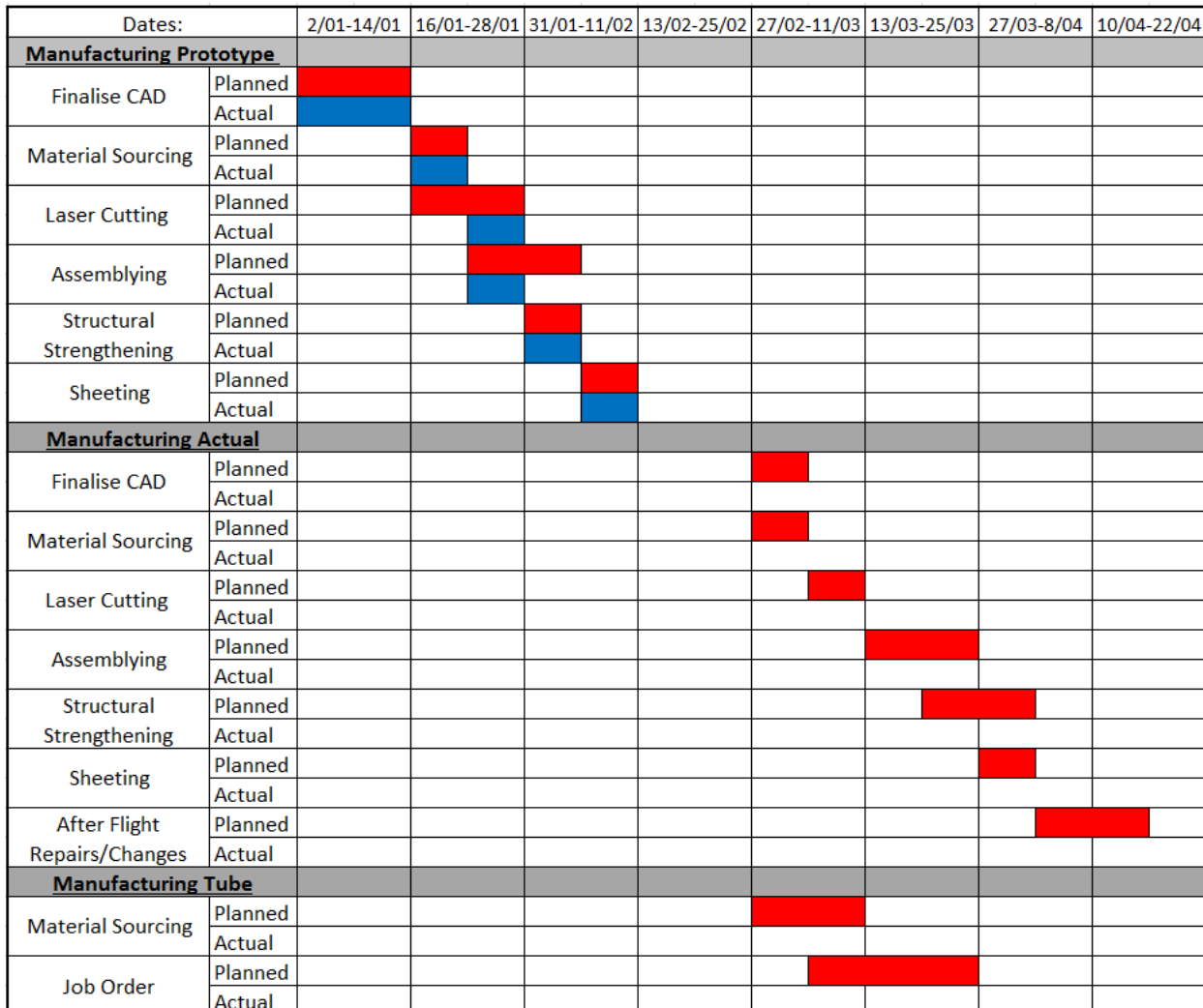


Figure 57: Manufacturing Milestone Chart

6.2. Material Selection

The hand launch requirement of this year's competition necessitates the need for a stronger structure to sustain the force exerted while hand launching. On the contrary, our RC plane still has to be light to minimize the RAC. To maximize these two conflicting parameters, we consider various structure that might give the best compromise.

The few structures considered were the use of carbon fiber, monocoque, formers & stringers, as well as the standard truss built up. As discussed in the concept design, a standard wood truss structure with features of former was chosen.

Type of wood	Directional Properties	Crushing Strength (MPa)
Balsa Wood	Yes	11.6
Basswood	Yes	32.6
Birch Plywood	No	41.0

Figure 58: Wood Data provided by Wood Database [5],[6] and Rochester Institute of Technology [7]

Thus, the principal material is balsa wood due to its light weight. Balsa wood is a relatively weak material, and it is not able to withstand certain forces that an RC plane is to experience in-flight or landing. Hence, secondary materials such as plywood and basswood are used strategically for components that are required to withstand greater stress forces.

During assembly, different material have to be joined. Hence various types of adhesives are needed. For joining wood to wood, cyanoacrylate will be sufficient to hold them in place. However, for joints that need to withstand more stress, wood glue would be used to keep them in place. For joining any other material to wood, epoxy is used as the adhesive material to provide the required strength.

6.3. Manufacturing Methods

The prototype was mainly laser cut or hand manufactured using hand tools such as drills, saws, and knives. Hot wire cutters were also used for our foam components.

Laser cutting of wood provides a superior dimensional accuracy and manufacturing speed when compared to hand cutting of wood. As such, most of our wooden parts are laser cut to shape.

In the prototype, some parts of the main frame were designed to have jigsaw fitting sides for easier assembly of parts as joints are now self-aligning. Furthermore, having the Jigsaw fitting also increases the area of glue joints thus strengthening the structure.

Through the laser cutting experience, some parts from the prototype would be more efficiently and accurately manufactured if it was made by additives using 3D printing technology. One such part was the flight mode alignment mechanism, which was proven to be hard to cut by laser cutting due to its thickness. Thus, it lost its dimensional accuracy after many cuts were made; this also will allow us to have a more sophisticated design.

Despite using laser cutting, there were some parts which were still hand cut, mainly the structure supporting pieces; this usually happens when the full assembly does not precisely follow the plan drawings. Other parts such as the stowing mechanism involved the use of hand tools and power tools for its manufacturing.

For the construction of the actual airplane, the majority of the parts will be done by laser cutting to reduce the time required for the production of the parts and allow more time for assembly. The steps will be similar to the prototype production, but changes will be implemented as we learned from the test trials and any identified inefficiencies. We will also be manufacturing spare parts and assembling them beforehand to make repairing the airplane easier when we are at the competition venue.

6.4. Manufacturing Components

The aircraft is categorized into different major components to facilitate manufacturing and assembly. The components include wing, fuselage, tail, landing gears and propulsion system. All the components are completed in the above specific order to ensure a smooth and continuous process from procurement to assembly. For all parts of the airplane, we will be using a top and side view drawings scaled to 1:1 ratio obtained from the 3D modeling. Construction of all parts will be done on a flat workshop table top. Upon completion of all assembly, the aircraft is then sheeted.

Aircraft parts	Subparts	Materials used
Wing	Wings	Balsa
	Landing skids	Plywood, Music wire
	Fuselage-wing joints	Plywood
Fuselage	Track	Basswood
	Body frame	Balsa
	Motor mount	Plywood
Empennage	Tail	Balsa, Plywood, Foam
	Landing skids	Plywood, Music wire
Reinforcements	-	Dental floss, Carbon fibre tubes
Adhesives	-	Cyanoacrylate, Wood Glue, Foam Glue, Epoxy

Figure 59: Manufacturing Components

6.4.1. Wings

Drawings are taped down on the workshop table top beneath a layer of clear book wrapping plastic which allows the drawings to be easily replaced. The first step we take for all construction is dry fitting which involves assembling parts over the drawings without gluing to allow for possible corrections. Since the wings are designed to have a polyhedral angle of 7.5 degrees, the wings will be constructed in 3 sections, center and sides. Each wing section will be assembled individually before attaching the side sections to the center section with basswood joiner and foam pieces to ensure that the side sections do not move about the center section.

For simplicity, only the center part of the wings will be explained in details. All parts of the wing are laser cut and glued into position using cyanoacrylate and epoxy. The center section is constructed first by aligning the lower horizontal spar on the drawings. The notches at the bottom of the ribs are glued to the lower spar with the use of an L-square ruler and accurately scaled drawings to ensure that each rib is perpendicular to the base of the wing and at regular intervals across the wing span. The upper spar is then glued into position at the notch at the top of the spar. Shear webs are the glued to the top and bottom spar.. Then the leading edge sheeting for the D-box are glued to the ribs, webs, and spars.



Figure 60: Main Wing Construction

The side wing sections are completed in a similar fashion and attached to the center section using basswood joiners. The required polyhedral angle of 7.5 degrees is measured using a protractor before gluing the joiners to the wing sections with epoxy. The joiner would have to handle a higher stress at the polyhedral hence the need for basswood and epoxy. Small pieces of foam are positioned into the gaps using foam glue to prevent movement of side sections about centre section of the wing.

6.4.2. Fuselage

The side and top view drawings of the fuselage were used to ensure that the trusses and bulkheads are placed in their correct arrangement. The bulkheads were made by gluing with 4 pieces of 1/32" balsa wood with wood. Holes were made on the 1/8" plywood motor mount using a bench drill to secure the motor to the fuselage nose.

Once the bulkheads are ready, the fuselage is assembled by gluing the trusses, bulkheads, and mechanism tracks together with wood glue and cyanoacrylate. Alignment tools such as L-square rulers and supporting blocks of woods are used to ensure that the bulkheads and tracks remain at 90deg to each other until the glue sets and cures. The Jigsaw features also ensure an accurate alignment during assembly.

6.4.3. Mechanism Tracks

The mechanism tracks are laser cut from a 1/8" basswood to create a strong unibody as the base of the fuselage.

6.4.4. Empennage

The trusses and plates for the entire empennage are laser cut to exact dimensions from a balsa plank of 3/16 in. Dry fitting shows that the assembly is as accurate as the drawings. The individual pieces are then glued on together using the drawings as reference. Gluing involves dripping cyanoacrylate to the joints. The whole plane of empennage is then rotated over before applying cyanoacrylate on the other side.

6.4.5. Reinforcements

Dental floss. All non-wood structures are secured using dental floss and a combination of adhesives. To secure the mechanism, the carbon fiber tube is tied to the 2 mm music wire with square lashing using several strands of dental floss . Cyanoacrylate is then applied over the dental floss to strengthen the joints. In the case of landing skids, the music wire is secured by weaving strands of dental floss in a criss-cross manner and applying cyanoacrylate. Due to the high impact force during landing, the joint is later reinforced using epoxy.



Figure 61: Dental Floss Reinforcement

Fiberglass. The nose of the fuselage is must be reinforced to withstand the stress imposed by the thrust of the motor during flight. The strength of basswood the trusses used in this section might not be sufficient to hold the nose in place when the motor is at full power. The fiberglass gussets are prepared by layering 3 layers of fiberglass sheets and a piece of Vanguard paper to add stiffness.



Figure 62: Fiberglass Gussets Reinforcement

7. Testing Plans

The following tests are conducted to ensure that the finished plane meets the required predicted flight requirement before the actual flight test. For the prototype aircraft, an additional test, destructive testing of wing, is implemented to check and confirm the rigidity and strength of the wing structure used.

7.1. Testing Schedule

Dates:		2/01-14/01	16/01-28/01	31/01-11/02	13/02-25/02	27/02-11/03	13/03-25/03	27/03-8/04	10/04-22/04
Prototype Plane									
Wingtip Load	Planned				■				
	Actual				■				
Propulsion System	Planned				■				
	Actual				■				
Landing Gear Impact	Planned				■				
	Actual				■				
Ground drop	Planned				■				
	Actual				■				
Flight Test	Planned				■				
	Actual				■				
Destructive Testing of Wing	Planned				■				
	Actual				■				
Actual Plane									
Wingtip Load	Planned						■		
	Actual						■		
Propulsion System	Planned						■		
	Actual						■		
Ground drop	Planned						■		
	Actual						■		
Landing Gear Impact	Planned						■		
	Actual						■		
Flight Test	Planned						■		
	Actual						■		

Figure 63: Testing Schedule

7.2. Testing Methods

7.2.1. Wingtip Load Test

To verify the structural strength of the wing, we perform a wingtip load test. This test is to ensure that the wing is capable of handling a load 2.5 times its maximum flying weight.

7.2.2. Propulsion System Test

This test involves turning the throttle to various settings while measuring with a multimeter the stable voltage and current drawn by the motor. Also, an electronic spring weighing scale was used to measure the thrust produced. This test is done to verify battery and motor performance by manufacturer data and ensure sufficient power and thrust.

7.2.3. Ground Drop Test

This year's competition requirement includes dropping the plane in a tube from a height of at least 12 inches from three different angles. As the tube for containing our plane is yet to be manufactured, we could not conduct the drop test exactly the way it would be done in the actual competition. We customized our

drop test accordingly, with the plane being dropped from the chest height of a person, which is approximately 47.2 inches.

7.2.4. Landing Gear Impact Test

The landing gear impact test is done to ensure the integrity of the plane's landing skids and subsequently the entire plane structure during landing. It is done by applying a horizontal force on the plane across tarmac road and grass patch to simulate landing during competition and test flight of our prototype respectively.

7.2.5. Destructive Testing of Wing

This test is to determine the maximum load that our wing structure can handle, which is useful in finding out the maximum G force our plane can take for a given flying weight.

7.2.6. Flight Test

The flight test is to verify the aircraft's airworthiness and to determine the actual mission performance of our plane. Furthermore, pilot feedback on the aircraft's stability and maneuverability will be useful for the next iteration of our design.

7.3. Pre-flight Checklist

Structural Integrity		Avionics	
Visually verify:		Check:	
Propeller mechanism secure		Radio range check	
Payload and electronic components secure		All wires plugged in and secure	
Hatch locked		Control surfaces have full authority (unhindered)	
Wings locked in flight position		Safety cut-off/arming switches work	
No loose or dangling features		Radio fail-safe mode activates and functions properly	
Propulsion System			
Check:			
Motor connected to main battery		Avionics battery fully charged	
Main battery fully charged			
On Flight Line			
Check:			
Pilot is ready to assume control		Wind direction	
Takeoff run-up area is clear of spectators and obstructions		Launcher is in position and ready to launch	

Figure 64: Pre-flight Checklist

8. Performance Results

8.1. Test Performance Results

8.1.1. Wing Tip Load Test Performance

Our plane is first loaded to its maximum takeoff weight and is then lifted by the wingtip. From observation, there are hardly any deflection or damage sustained by the wings. Therefore, we conclude that our aircraft can handle 2.5 G of load



Figure 65: Wing Tip Load Test

8.1.2. Propulsion System Test Performance

Propeller Dimensions	12" x 8"					11" x 8"				
Throttle Setting (%)	0	25	50	75	100	0	25	50	75	100
Voltage (V)	12.4	12.5	11.9	11.3	10.9	11.5	11.4	11.1	10.8	10.6
Current (A)	0.2	5.1	19.6	31.9	35.7	0.1	5.4	16.5	27.2	31
Power (W)	2.48	63.8	233	360	389	1.15	61.6	183	293	328
Power Loading (W/lb)	0.66	17	62	96	104	0.31	16	49	79	88
Thrust (g)	0	265	685	1245	1650	0	255	570	1055	1035

Figure 66: Propulsion System Testing

The motor demonstrated that it could provide sufficient power for the airplane to achieve the desired performance. The 11" x 8" propeller was selected as it produces sufficient thrusts for our desired aircraft performance

8.1.3. Destructive Testing of Wing Results

To determine the maximum extent of our wing's structural strength, the wing is loaded until it fractures. The plane is first supported on both tips. Weights are then added on the fuselage until any sign of damage is first observed in the wing structure. In this test, crack is experienced at a deflection of 2.7cm.



Figure 67: Destructive Testing of Wing

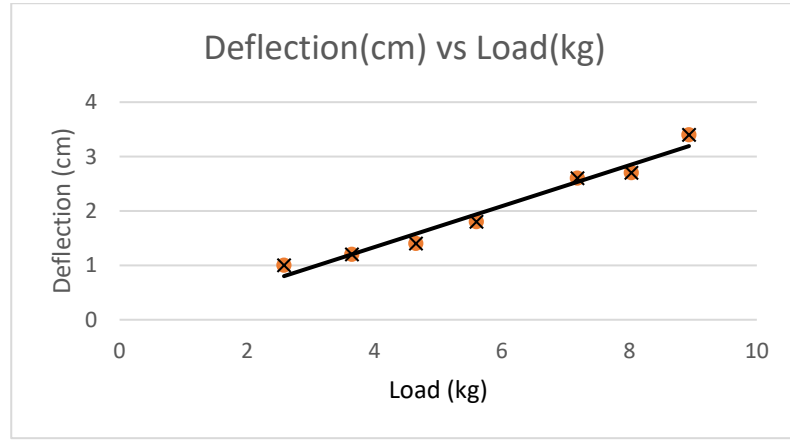


Figure 68: Wing Deflection Graph

The wing of the aircraft could handle weights up to 8 kg before any damage was observed. The deflection against load graph appeared as a linear line, as shown in the figure above; this shows that our wing could handle a payload much higher than the current maximum of 3 pucks.

8.1.4. Ground Drop Test Performance

The test will determine if the plane has the structural strength to survive a landing without sustaining damages. We observe no damage in our plane after the drop test. With the aid of cushioning from the tube during the actual competition's drop test, the aircraft should be able to survive the test. For the drop test that lands on the tube's end, the highest stressed joint in the drop test is expected to be the joint between the wing and the plane's fuselage due to the difference in the length of the fuselage and the wing in the stowed position. All other parts would be cushioned from the impact by the foam within our tube.



Figure 69: Ground Drop Test

8.1.5. Landing Gear Impact Test Performance

Our landing skid failed the initial test; this is because the landing skids have hooks pointing towards the nose of the plane. When the landing skids slide across the ground, the hooks latch into the soil, causing great traction on the aircraft. A hollow rubber tube was later added to the landing skid to reduce the possibility of the hooks digging into the ground. Subsequent tests show that although the tube mitigates the issue, it does not eliminate it. In future designs, we will point the landing skids backward so that the aircraft can slide on the ground instead of abruptly decelerating upon landing.



Figure 70: Landing Skids with Tubing

8.2. Flight Test Results

8.2.1. Hand Launch Practice Test

The competition this year added complexity by including the hand launch requirement. At least one of our student member needs to be familiar with hand launch techniques. To ensure that our thrower has the necessary skill and confidence to hand launch an RC plane, we purchased an off-the-shelf Funter foam plane to practice our throwing skills. The Funter is made of foam which is resistant to damage incurred from practice, and easy to repair too.

The table below compares the parameters of the two planes.

Parameters	300301 Funter ARF Version	Our prototype (Calculated)
Wingspan	1650 mm	1200 mm
Length	1159 mm	1130 mm
Empty Weight	1050 grams	1165 grams

Figure 71: Funter Plane Comparison



Figure 72: Practicing with the Funter Plane

As the weight of 300301 Funter ARF version is lower than our actual plane's weight, we added our own payload to the Funter. We started off practicing with the original weight, which is 1050g and subsequently increasing the weight until it reaches 1500g.

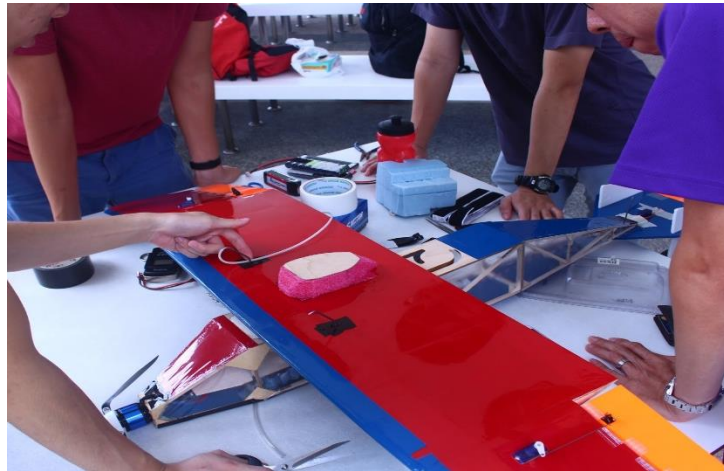
Through analyzing our video of the hand launch, we calculated that the maximum throwing speed is slightly above 10 meters per second. Through using a high-speed camera (240 frames per second), we could analyze the video frame by frame to track our plane's movement. We drew equally spaced marking on the belly of the aircraft for additional reference to track the aircraft's movement. Note that the thrower ran while hand launching.



Figure 73: 10cm Marking on the Funter

8.2.2. Prototype Maiden Flight Test

The prototype aircraft's original design is to have a foam block between and below the two wing roots. Note that the position of the center of gravity (CG) lies slightly in front the foam block. This foam block is the grip for hand launch.



Our plane crashed shortly after being hand launched due to excessive roll of the aircraft before leaving the thrower's hand. The plane suffered a broken epoxy joint between the carbon fiber tube and the wing's rib. Large rubber bands and duct tape were used to secure the wing and the fuselage in position before we continue with subsequent flight test.

Through our first flight attempt, we noted that the compressibility of the foam not only makes it difficult to control the roll of the aircraft during the hand launch, but it also makes the thrower less aware of the direction of which the aircraft leaves the hand. By analyzing our video, we calculated the hand launch speed is slightly above 9 m/s. Do note that the thrower ran while hand launching the plane.

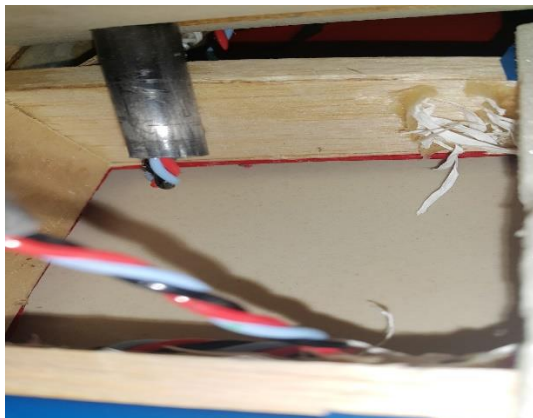


Figure 74: Broken Carbon Fiber Tube



Figure 75: Failed Hand Launch



Figure 76: Prototype Fastened with Tape After Crash

Due to our low-wing configuration, the prototype's wing is below the CG, and the thrower could not grip the fuselage directly below the CG. The thrower feedbacked that being unable to grip the plane at the CG increases the instability of the plane during the hand launch process. The thrower now grips the plane with two hands at two separate position, one in front of the CG and the other behind. This grip allowed a more controlled throw, significantly increasing the chance of a successful throw.

8.2.3. Prototype Subsequent Flight Test

The prototype plane is repaired on the spot and proceed for subsequent hand launches which proved to be successful with the aircraft flying smoothly in the air. The pilot was able to control the yaw, pitch, and roll of the plane, showing that the control surfaces are sufficiently large to give the pilot good control of the plane. However, Dutch roll was observed during the flight, suggesting that the lateral stability is too strong relative to the directional stability. By analyzing our flight video, we calculated that our plane's flight speed exceeded 18.6 m/s. However, the actual flight speed is not able to determined accurately due to the limitation of our measurement tool. The required running distance is 20m.



Figure 77: Prototype Plane Coming in for Landing



Figure 78: Prototype Plane in Cruising

8.3. Area of Improvements

The foam grip will be removed and the fuselage will be used as the grip instead, which allows better control of hand launches by the thrower. The dihedral wing can generate unwanted roll when thrown with a yaw angle. Therefore, the polyhedral angle was too high. As such, we have decided to further reduce our polyhedral angle from 15 degrees in our prototype to 7.5 degrees in our final design, resulting in an effective dihedral angle of 4.93 degrees.

During the first crash, the carbon fiber tube -wing connection was the one that failed first. Therefore, in our subsequent design, we will further strengthen that joint.

The flight tests also reveal a tendency for the airplane to pitch down in flight, requiring a constant up elevator trim. As such, the horizontal stabilizers for the next aircraft will be designed with a small negative angle of incidence.

9. Bibliography

- [1] Anderson Jr, J. D., "Fundamentals of Aerodynamics," 5th ed., 2010.
- [2] Current Results, "Humidity Levels in Arizona During April," Weather and Science facts [online database], <https://www.currentresults.com/Weather/Arizona/humidity-april.php> [retrieved 21 February 2017]
- [3] Kermode, A. C., "Mechanics of flight," 9th ed., 1989. ISBN 10: 058242254X
- [4] The Engineering Toolbox, "Altitude above Sea Level and Air Pressure," Atmospheric pressure data [online database], http://www.engineeringtoolbox.com/air-altitude-pressure-d_462.html [retrieved 21 February 2017]
- [5] The Wood Database, "Balsa," Wood Database [online database], <http://www.wood-database.com/balsa/> [retrieved 21 February 2017]
- [6] The Wood Database, "Basswood," Wood Database [online database], <http://www.wood-database.com/basswood/> [retrieved 21 February 2017]
- [7] Rochester Institute of Technology, "Plywood Materials," School Portal [open source database] <http://edge.rit.edu/edge/P14418/public/4-Subsystems%20Design/Plywood%20Materials.pdf> [retrieved 21 February 2017]